PWA FR-1308
30 MAR 1965

QUARTERLY PROGRESS REPORT NO. 3

INVESTIGATION OF COMBUSTION INSTABILITY WITH LIQUID OXYGEN AND LIQUID OR COLD GASEOUS HYDROGEN PROPELLANTS

PHASE II

Prepared By: Wm. J. McAnally
W. J. McAnally

Approved By: J. Emory
J. Emory
Assistant Project Engineer

Burton A. Jones
Burton A. Jones
Program Manager

Pratt & Whitney Aircraft DIVISION OF UNITED AIRCRAFT CORPORATION

FLORIDA RESEARCH & DEVELOPMENT CENTER

Printed in the United States of America

ABSTRACT

32723

Twenty-five tests with the 1 x 5-inch two-dimensional slab motors were conducted during the third quarter. Initial analysis of test results confirms the previously observed stabilizing trends of increased hydrogen temperature, increased injection momentum ratio, and increased chamber contraction ratio. Detailed analysis will be presented in the final report.

author

CONTENTS

ILLUSTRATIONS

ILLUSTRATIONS (CONTINUED)

ILLUSTRATIONS (CONTINUED)

SECTION I
INTRODUCTION

During this report period, experimental effort was continued in accordance with the objectives outlined in Quarterly Progress Report No. 1 (Reference 1). Testing of all but one slab motor configuration was completed. The remaining configuration will have a concentric sheet-type injector. Hardware for the sheet injector was received and assembly of the final slab motor configuration with this injector was in progress at the end of the report period. It is currently planned to omit the nominal 5-inch diameter chamber tests in lieu of an equivalent number of 1 x 5-inch slab motor tests, pending authorization from the Contracting Officer. The plan is mutually agreeable to the NASA Technical Director and Pratt & Whitney Aircraft because the additional 1 x 5-inch slab motor test results will be of more value to the overall program objective.

The program schedule showing progress achieved to date is presented in figure I-1. Figure I-2 presents the test matrix defining completed and remaining configurations to be tested. As stated in previous reports, in many instances more tests than the number shown were obtained for a given configuration.

This progress report presents a brief description of test equipment and procedures, discussion of the results of tests conducted during this quarter, and up-dated data correlations showing the effect of the program variables on stability limits.

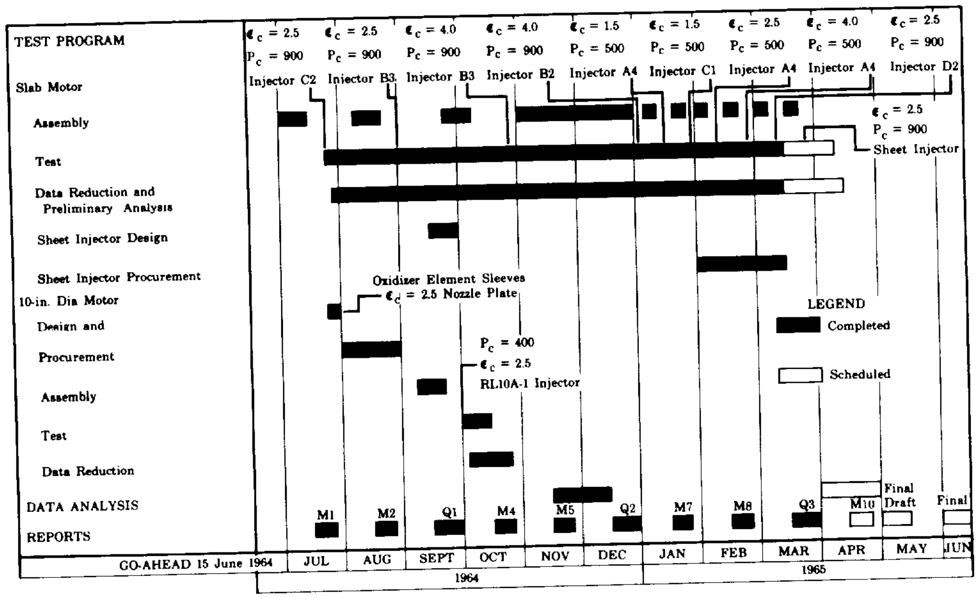

Figure I-1. Combustion Instability Program Schedule FD 9437B

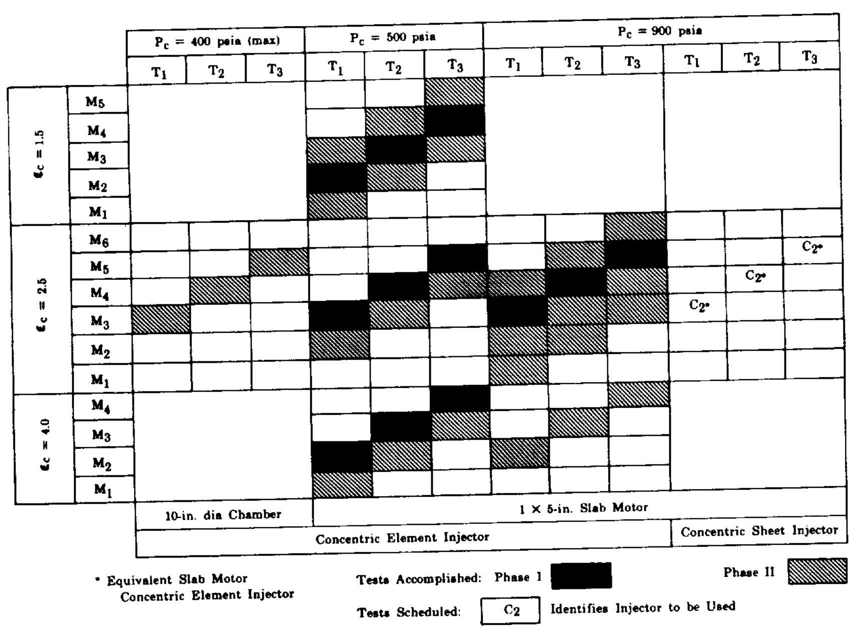

Figure I-2. Test Matrix

FD 10432A

SECTION II
TEST EQUIPMENT AND PROCEDURE

Test equipment, explosive pulse system, and data processing systems used during this report period were the same as those described in detail in Quarterly Progress Report No. 1 (Reference 1). A description of the test hardware and minor changes in test procedure are presented below. A simplified propellant flow diagram is also presented to identify data measurement locations.

A. TEST HARDWARE

A schematic of the 1 x 5-inch slab motor showing the location of the high-frequency response Kistler chamber-pressure transducers and the explosive pulse units is presented in figure II-1. A list of dimensions is contained in table II-1 for the 18 concentric element injector configurations.

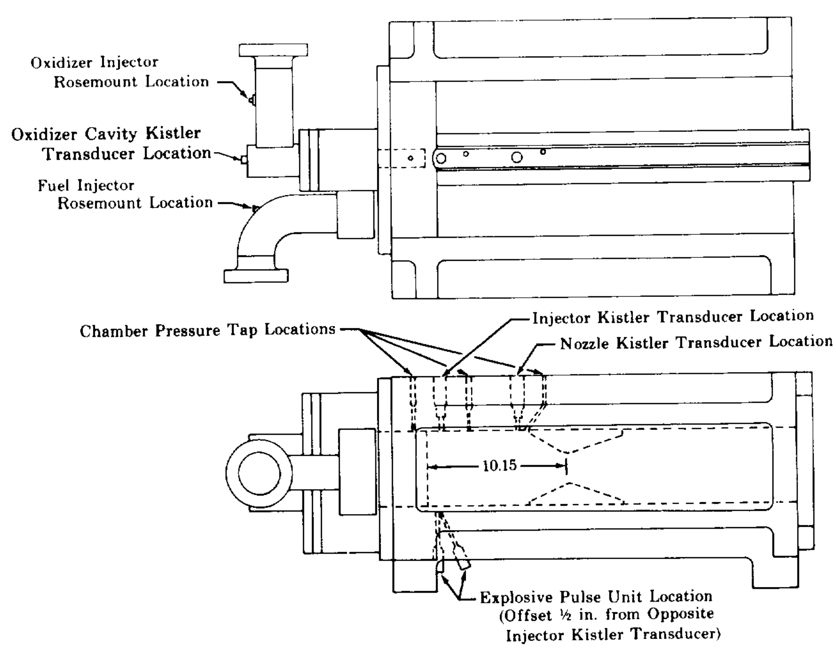

Figure II-1. 1 x 5-Inch Slab Motor Instrumentation

FD 9434A

Table II-1. Injector Configurations

Slab Motor Injectors, 18 Elements		Designation
Fuel Orifice Annulus, in.		
ID	OD	
0.182	0.1935	1
0.182	0.2015	2
0.182	0.2113	3
0.182	0.2373	4
Oxidizer Orifice Diameter, in.		
0.0673		A
0.0847		B
0.0997		C
0.1331		D
Sheet Injector		
Sheet injector areas will be the same as injector configuration C2.		

The revised injector Rigimesh face attachment described in Quarterly Progress Report No. 2 (Reference 2) has been entirely satisfactory in all tests conducted with the new design. Modification of the second slab motor was completed early in the quarter. Availability of the two slab motors, shown in figure II-2, has made possible the increased testing rate that has enabled the program to return to schedule.

The sheet injector for the slab motor was designed and procured during this report period. It consists of a single axial liquid oxygen injection slot surrounded by a concentric hydrogen injection slot that is inclined 45 degrees inward from the axial direction. A cutaway illustration of this injector is shown in figure II-3 and a photograph of the injector face in figure II-4. The injection areas are the same as the C2 concentric element injector.

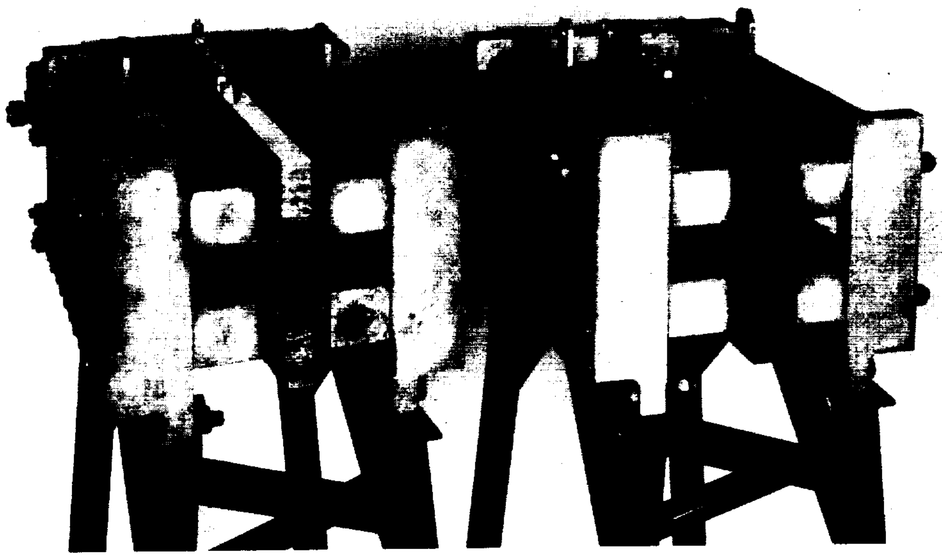

Figure II-2. Slab Motors FE 48817

B. TEST PROCEDURE MODIFICATION

Slab motor tests were conducted using the procedure described in Quarterly Progress Report No. 2 (Reference 2). Improvements were made to the abort system to preclude the type of hard start that occurred during the second quarter. Cold flows were conducted prior to firing each configuration to determine proper low-chamber-pressure abort switch setting. A burnwire ignition abort system was also incorporated. A review of test data indicates that these abort systems would have safely terminated the test if an ignition failure or absence of proper chamber pressure rise had occurred during any test conducted this report period.

Following test 52.01, test duration was reduced from 1.5 to 1.0 seconds to lessen the probability of hardware deterioration. The explosive pulse charges were fired at 0.50 and 0.75 seconds.

FD 11616

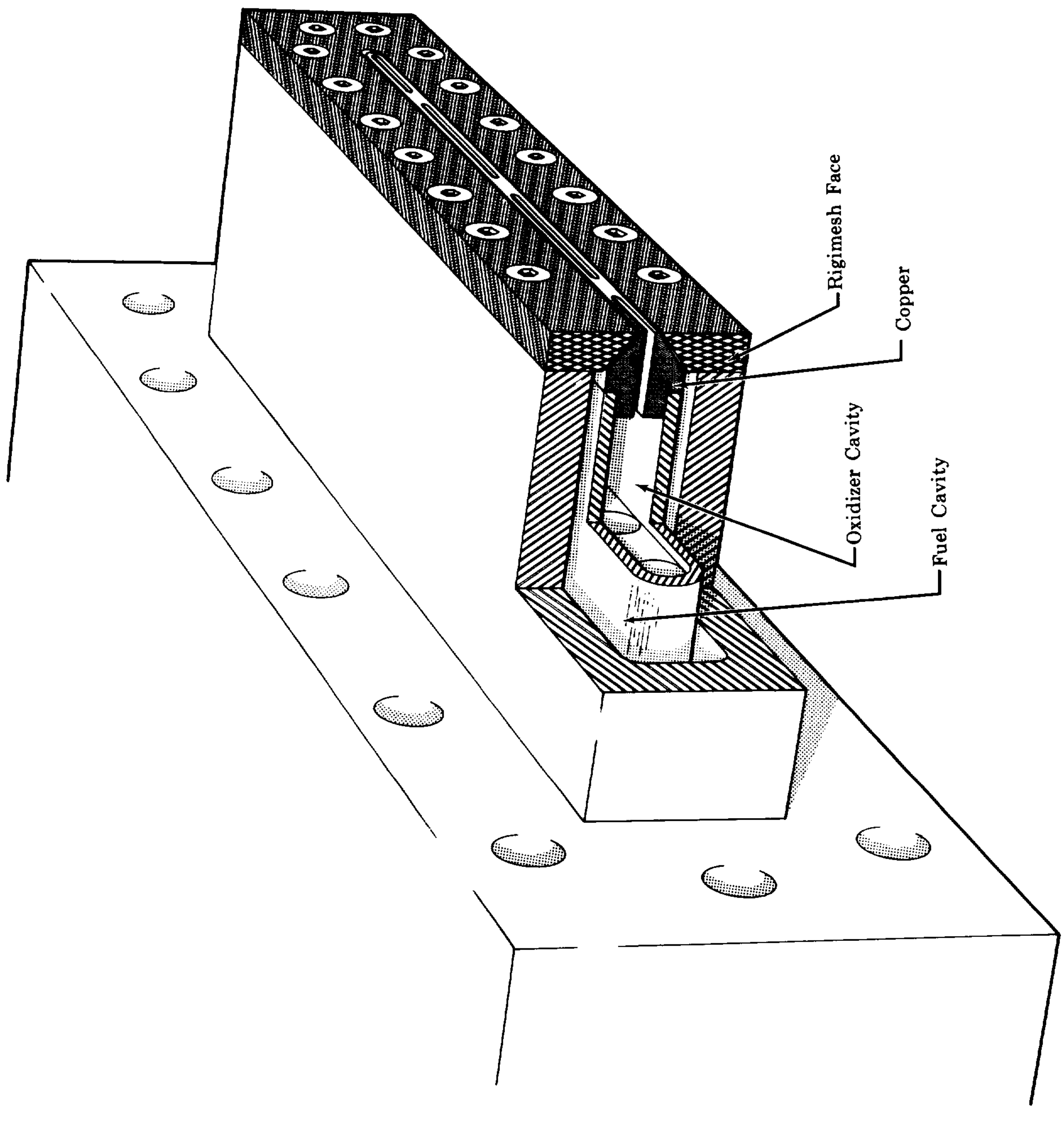

Figure II-3. Cutaway of Sheet Injector

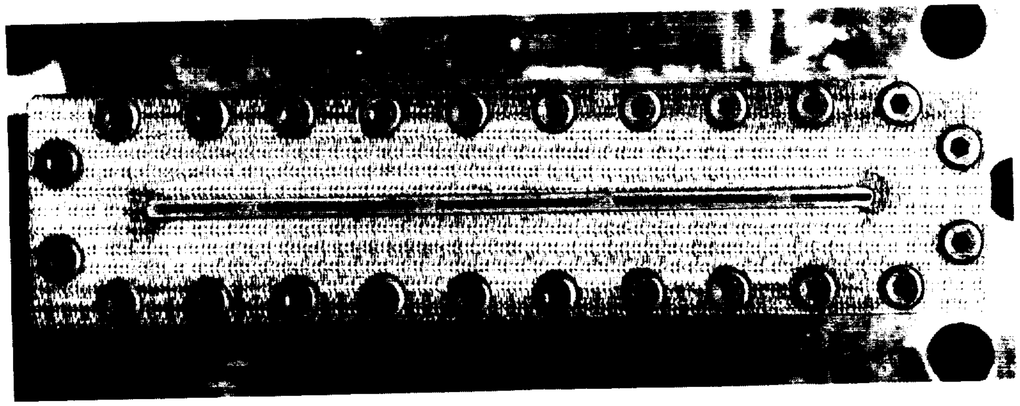

Figure II-4. Sheet Injector FE 49529

A propellant flow diagram of B-8 test stand is presented in figure II-5. The gaseous hydrogen-liquid hydrogen mixing system and the location of test data instrumentation are shown. During tests with low hydrogen momentum injectors, the rig fuel inlet line diameters were reduced to provide increased system pressure drop and, therefore, less flow variation because of chamber pressure variation. The liquid oxygen supply line had sufficient pressure drop to prevent this flow variation, although low oxidizer momentum injectors still had a chugging tendency.

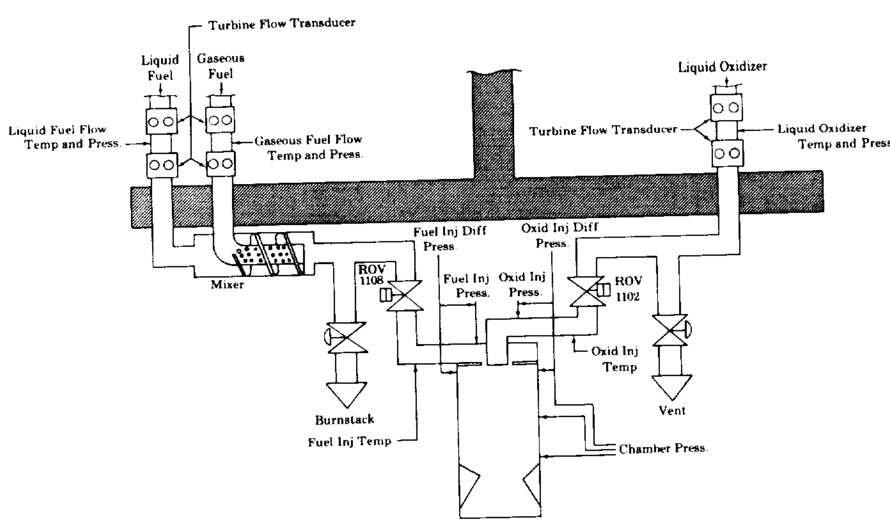

Figure II-5. B-8 Combustion Instability Test Stand Schematic FD 10431

SECTION III
TEST RESULTS

A. GENERAL

Twenty-five tests were conducted with two slab motors during this report period. A wide range of test variables was covered using six injector configurations. The results of the twenty-five tests are summarized in table III-1.

The following technical discussion of the results of individual tests describes the pertinent test parameters and interprets the Kistler Chamber pressure transducer data. Condensed Kistler transducer data transcriptions are presented for most tests. Pressure amplitude vs frequency distribution plots and partial Kistler data transcriptions with expanded time scales showing detailed wave form are presented for selected tests.

B. TECHNICAL DISCUSSION

1. Injector Configuration B2 Tests (Contraction Ratio 4.0:1)

Five test firings were conducted with injector configuration B2 at 900 psia nominal chamber pressure using the 4.0 to 1 contraction ratio nozzle. (Injector has a fuel orifice annulus 0.182-in. ID and 0.201-in. OD and 0.084-in. oxidizer orifice diameter.) A test duration of 1.5 seconds was programed at full chamber pressure. Condensed oscillograph transcriptions of chamber Kistler transducer data are presented in figure III-1, for tests 48.14, 49.01, 50.01 and 52.01.

Test No. 48.14 was conducted at a fuel injection temperature of 65°R. The first pulse triggered combustion instability, which continued until shutdown. An expanded oscillograph trace (figure III-2) shows the 9.0-grain explosive pulse triggered combustion instability. This trace indicates the instability to be intermediate-frequency coupled with high-frequency. The pressure amplitude vs frequency distribution plot (figure III-3) indicates maximum peak-to-peak pressure amplitudes occurring at approximately 650 cps and 6200 cps. The latter frequency corresponds to the chamber first transverse acoustic mode. The pressure amplitude vs frequency distribution plot of data from the Kistler transducer located in the oxidizer cavity shows negligible coupling with combustion instability in the chamber. (See figure III-4.)

Table III-1. Slab Motor Te[illegible]t

Test Number	ϵ_c	Injector Configuration	Chamber Pressure, psia	Total Propellant Weight Flow, lb/sec	Overall Mixture Ratio	Fuel Injection Temperature, °R	Oxid[illegible] Injec[illegible] Temper[illegible] °R
48.01	4.0	B2	850	4.60	3.60	65	20[illegible]
49.01	4.0	B2	882	4.93	5.94	67	20[illegible]
50.01	4.0	B2	840	5.31	9.40	70	20[illegible]
51.01	4.0	B2	935	5.85	10.04	72	19[illegible]
52.01	4.0	B2	905-875	5.68-5.65	5.75-10.50	76-82	219-[illegible]
53.04	1.5	A4	675	8.41	2.35	61	21[illegible]
54.01	1.5	A4	533	7.56	4.76	63	20[illegible]
55.01	1.5	A4	556	7.49	4.47	63	2[illegible]1
56.01	1.5	A4	568	7.87	4.82	64	1[illegible]9
57.01	1.5	A4	454-507	7.06-7.31	10.0-6.40	148-97	214-[illegible]
58.04	1.5	C1	548	7.04	3.79	61	2[illegible]9
59.01	1.5	C1	573	7.13	3.81	62	2[illegible]8
60.01	1.5	C1	552	6.97	4.23	62	2[illegible]6
61.01	1.5	C1	525	6.82	5.21	87	2[illegible]9

1. Spontaneous instability from start-tra[illegible]
2. Spontaneous burst of instability
3. Sustained instability triggered by ex[illegible]

ults

Injection Velocity Ratio	Injection Momentum Ratio	Pulse Method	Instability Rating	Remarks
2.84	0.79	9.0-and 14.4-Grain Explosive	3	First pulse triggered intermediate-frequency coupled with high-frequency instability until shutdown.
2.12	0.36	9.0-and 14.4-Grain Explosive	5	First pulse was quickly damped. Second pulse triggered 400 cps instability but no high-frequency instability.
1.45	0.15	9.0-and 14.4-Grain Explosive	5	Completely stable, both pulses were quickly damped.
1.35	0.13	9.0-and 14.4-Grain Explosive	5	Only first pulse fired, test appeared to have been stable.
1.77-2.74	0.31-0.26	9.0-and 14.4-Grain Explosive	2-3	Bursts of high-frequency instability early in test. First pulse was quickly damped but a short burst of high-frequency instability occurred 0.2 sec later. Second pulse triggered intermediate-frequency coupled with high-frequency instability.
1.49	0.63	9.0-Grain Explosive	1	High-frequency instability from start-transient until shutdown.
1.08	0.23	9.0-Grain Explosive	1	High-frequency instability from start-transient until shutdown.
1.14	0.26	9.0-Grain Explosive	1	High-frequency instability from start-transient until shutdown. Explosive pulse unit did not operate.
1.09	0.23	9.0-Grain Explosive	1	High-frequency instability from start-transient until shutdown.
1.85-1.95	0.18-0.30	9.0-Grain Explosive	5-1	High-frequency instability from start-transient, stopped as fuel temperature increased. After fuel temperature had reached a peak and was decreasing high-frequency instability resumed until shut-down.
9.25	2.44	9.0-and 14.4-Grain Explosive	3	Test began with chugging. Second pulse triggered sustained high-frequency instability.
9.05	2.38	9.0-and 14.4-Grain Explosive	5	First pulse triggered sustained chugging throughout test. Second pulse was quickly damped.
8.53	2.02	9.0-and 14.4-Grain Explosive	3	Test began with chugging. First pulse triggered sustained high-frequency instability.
9.87	1.90	9.0-and 14.4-Grain Explosive	5	Chugging sustained from start of test. First pulse did not fire. Second pulse was quickly damped.

ıstability Rating

:

4. Bursts of instability triggered by explosive pulse
5. Stable, no high-frequency combustion instability

ɜ pulse

Table III-1. Slab Motor Test R[illegible]

Test Number	ϵ_c	Injector Configuration	Chamber Pressure, psia	Total Propellant Weight Flow, lb/sec	Overall Mixture Ratio	Fuel Injection Temperature, °R	Oxid[illegible] Injec[illegible] Temper[illegible] °R
62.01	1.5	C1	560	7.34	5.61	88	20
63.01	1.5	C1	591	7.54	4.54	62	20
64.01	2.5	A4	510-502	5.04-4.36	4.49-4.58	69-70	233-[illegible]
65.01	2.5	A4	485	4.40	6.84	72	21[illegible]
66.01	2.5	A4	512	4.80	4.61	65	2[illegible]
67.01	2.5	D2	876	8.02	3.84	59	2[illegible]
68.01	2.5	D2	863-809	10.10-10.93	4.72-4.94	61-59	207-1[illegible]
69.05	4.0	A4	510	2.75	4.25	70	2[illegible]
70.02	4.0	A4	532	2.74	4.95	68	2[illegible]
71.03	4.0	A4	525	2.52	5.12	71	2[illegible]
72.01	4.0	A4	534	2.62	5.00	69	2[illegible]

1. Spontaneous instability from start-tr[illegible]
2. Spontaneous burst of instability
3. Sustained instability triggered by ex[illegible]

s (Continued)

Injection Velocity Ratio	Injection Momentum Ratio	Pulse Method	Instability Rating	Remarks
10.05	0.792	9.0-and 14.4-Grain Explosive	5	First pulse triggered sustained chugging. Second pulse was quickly damped.
7.94	1.75	9.0-and 14.4-Grain Explosive	5	Both pulses triggered chugging that tended to damp out.
1.29-1.37	0.288-0.299	9.0-and 14.4-Grain Explosive	2-5	Test started with sustained 550 cps intermediate-frequency instability that burst into intermediate combined with high-frequency instability until stopped by the first pulse. Intermediate-frequency continued until shutdown. Second pulse was quickly damped.
1.38	0.202	9.0-and 14.4-Grain Explosive	2	Test started with sustained 550 cps intermediate-frequency. Two short bursts of high-frequency combined with intermediate-frequency instability prior to first pulse. Another short burst of high-frequency combined with intermediate-frequency instability between first and second pulses.
0.971	0.210	9.0-and 14.4-Grain Explosive	2	Test began with high-frequency combined with 550 cps intermediate-frequency instability that damped itself prior to the second pulse. The first pulse did not fire. A short burst of high-frequency combined with intermediate-frequency instability occurred 80 ms after the second pulse.
5.27	1.37	9.0-and 14.4-Grain Explosive	5	Severe chugging sustained from start of test. The first pulse was quickly damped. The second pulse did not fire.
4.82-5.55	1.02-1.13	9.0-and 14.4-Grain Explosive	5-2	Severe chugging sustained from start of test. Neither pulse fired. High-frequency instability began spontaneously near end of test. Throat partially eroded.
1.55	0.364	9.0-and 14.4-Grain Explosive	5	600 cps intermediate-frequency instability was sustained from start of test. Both pulses were quickly damped.
1.61	0.325	9.0-and 14.4-Grain Explosive	5	600 cps intermediate-frequency instability sustained from start of test. Both pulses were quickly damped.
1.51	0.295	9.0-and 14.4-Grain Explosive	5	650 cps intermediate-frequency instability sustained from start of test. Both pulses were quickly damped.
1.90	0.380	9.0-and 14.4-Grain Explosive	5	650 cps intermediate-frequency instability sustained from start of test. Both pulses were quickly damped.

ıstability Rating

:

4. Bursts of instability triggered by explosive pulse
5. Stable, no high-frequency combustion instability

: pulse

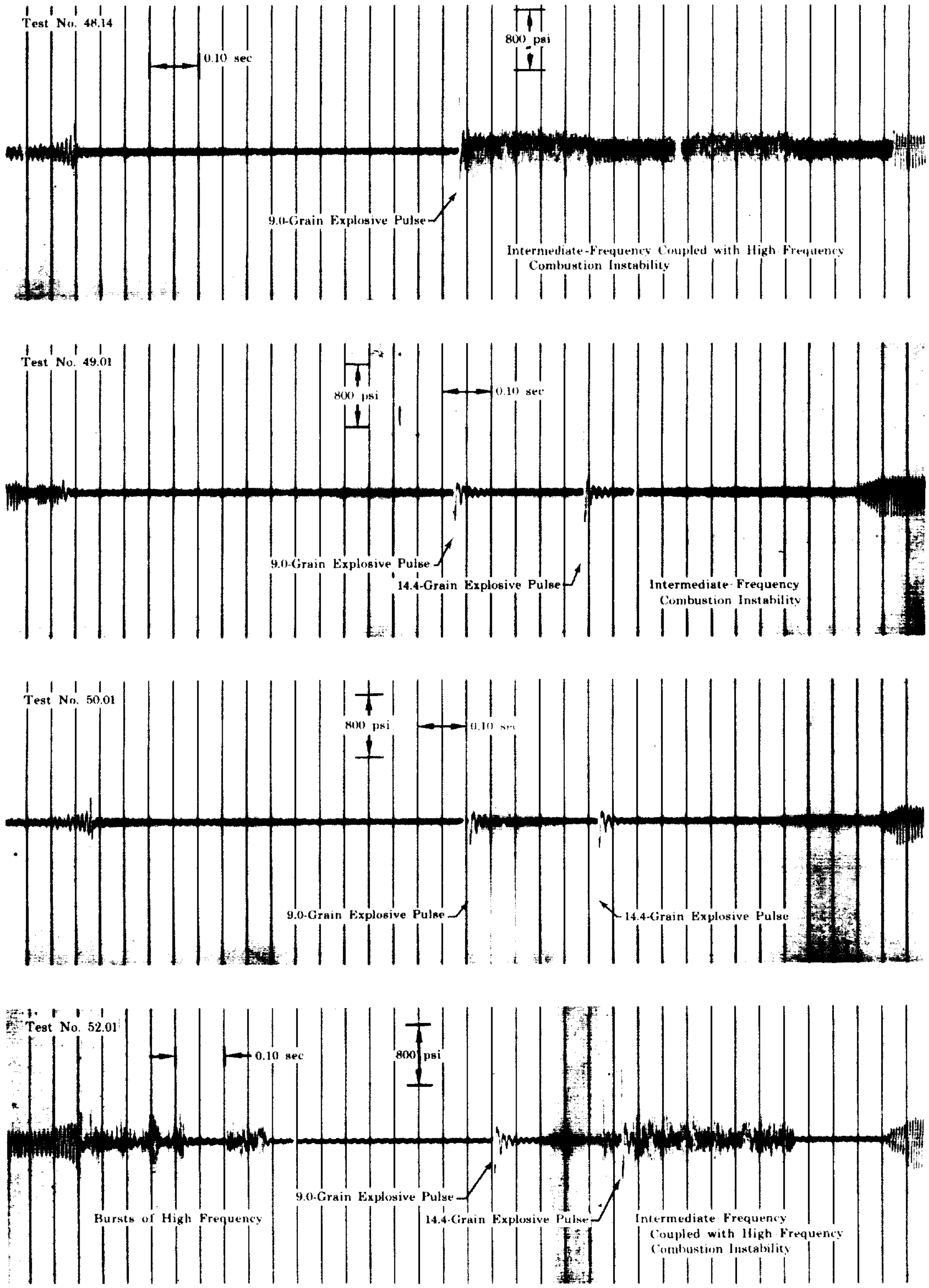

Figure III-1. Kistler Transducer Data from Tests No. 48.14, 49.01, 50.01, and 52.01 FD 11650

FD 11641

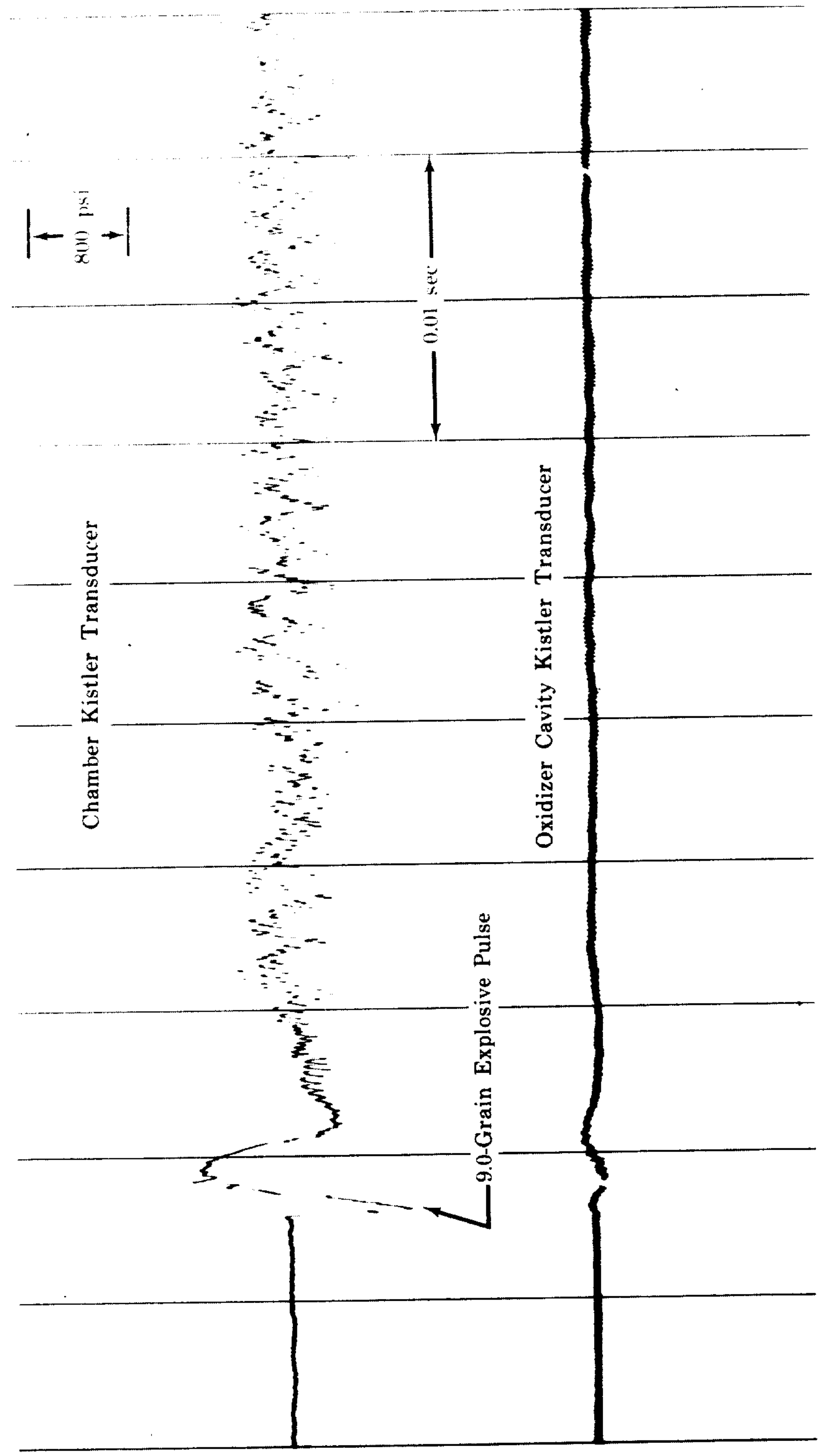

Figure III-2. Kistler Transducer Data from Test No. 48.14 Showing Combustion Instability Triggered by Explosive Pulse

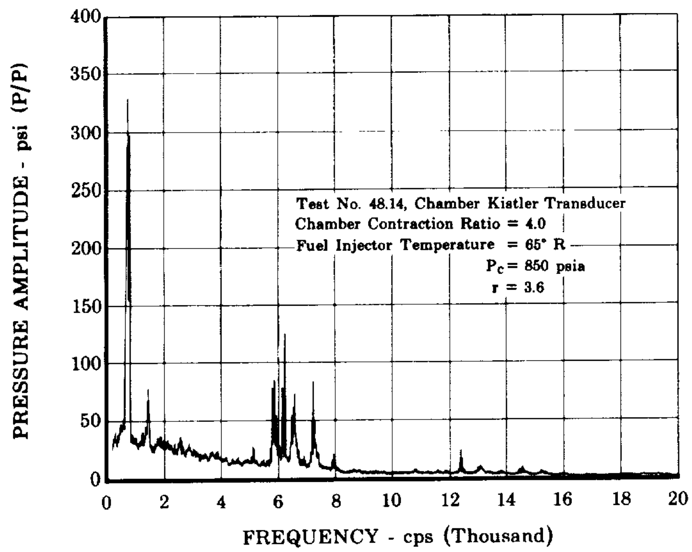

Figure III-3. Pressure Amplitude vs Frequency, Test No. 48.14, Chamber Kistler Transducer FD 11610

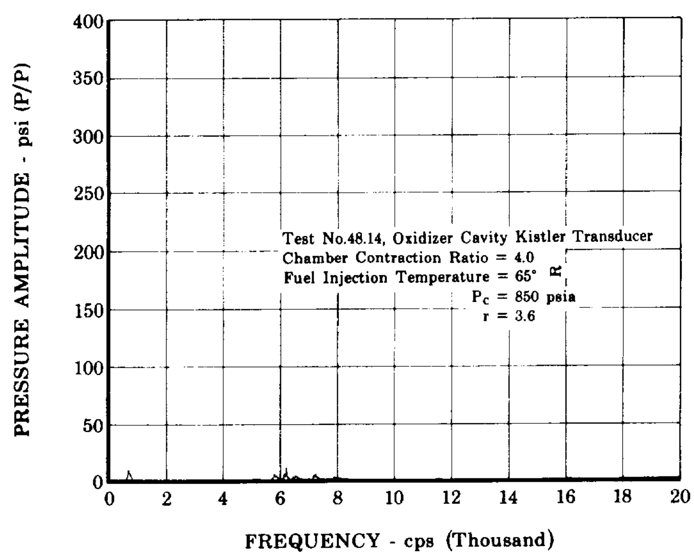

Figure III-4. Pressure Amplitude vs Frequency, Test No. 48.14, Oxidizer Cavity Kistler Transducer FD 11608

Test No. 49.01 was conducted at a fuel injection temperature of 67°R. The 9.0-grain explosive pulse was quickly damped, however, the 14.4-grain explosive pulse triggered a low-amplitude 400-cps instability that continued until shutdown.

Test No. 50.01 was conducted at a fuel injection temperature of 70°R and was entirely stable. Both explosive pulses were quickly damped.

Test No. 51.01 was conducted at a fuel injection temperature of 72°R with no high-frequency Kistler transducer tape data obtained. The response of the regular pressure transducer oscillograph traces indicated that only the 9.0-grain explosive pulse fired and that it was quickly damped. Comparing these data with those from other known stable tests, it may be concluded that there was no combustion instability.

During the last test of this series, test No. 52.01, fuel injection temperature varied from 76° to 82°R as mixture ratio ranged from 5.75 to 10.50. Two mixture ratio data points are presented for this test in table III-1. It is suspected that the mixture ratio variation was caused by pieces of injector internal Kel-F insulation breaking and partially blocking the fuel flow. The test began with spontaneous bursts of combustion instability for the first 1/2 second. The first pulse was quickly damped; however, 0.2 seconds later a burst of combustion instability occurred. An expanded oscillograph trace (figure III-5) shows combustion instability triggered approximately 25 ms after the 14.4-grain explosive pulse. The instability is indicated to be intermediate-frequency coupled with high-frequency. The pressure amplitude vs frequency distribution plot (figure III-6) indicates maximum peak-to-peak pressure amplitudes occurring at approximately 600 cps and 6100 cps. The pressure amplitude vs frequency distribution plot of data from the Kistler transducer located in the oxidizer cavity shows negligible coupling with combustion instability in the chamber. (See figure III-7.)

It was observed that oxidizer cavity pressure oscillations generally followed the chamber pressure oscillations, but with much reduced amplitude. Oxidizer cavity Kistler transducer data were recorded and monitored for all the following tests, but only unusual or significant results will be reported.

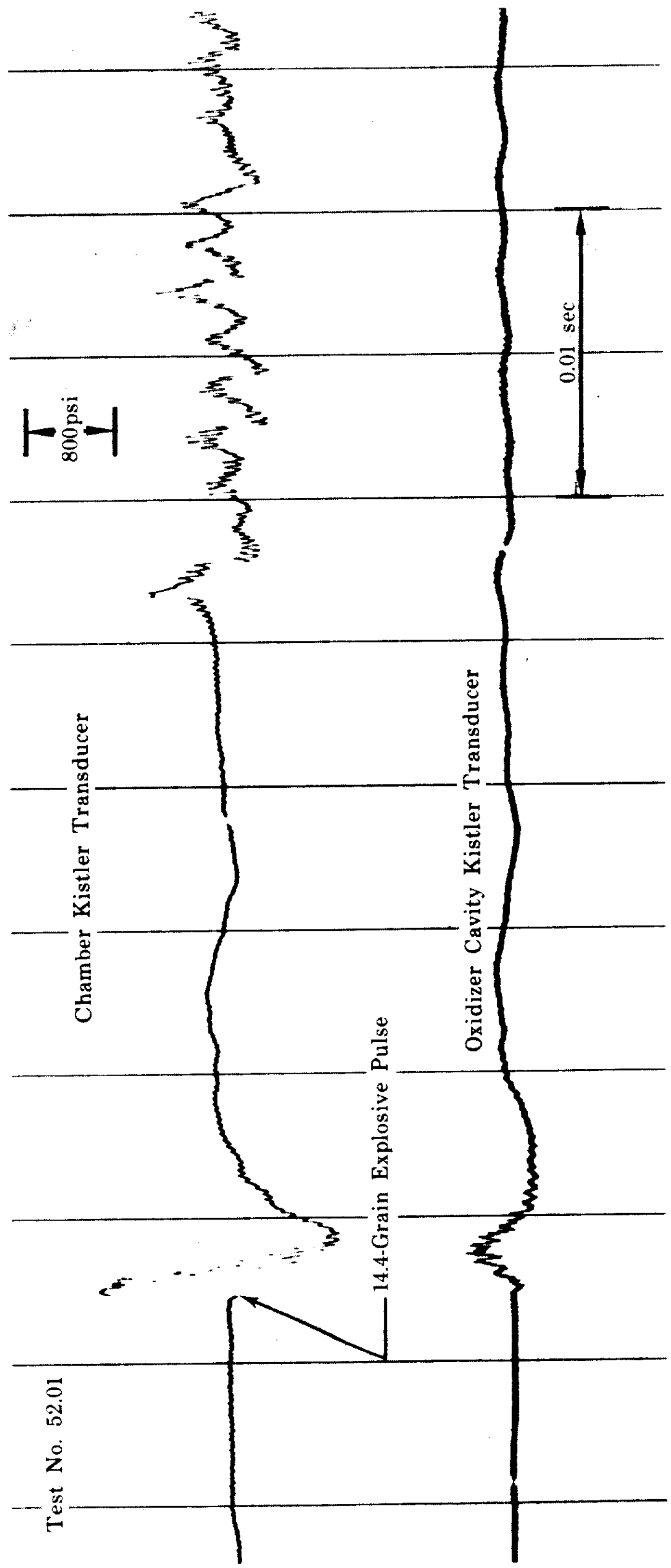

FD 11644

Figure III-5. Kistler Transducer Data from Test No. 52.01 Showing Combustion Instability Triggered 25 ms after Explosive Pulse

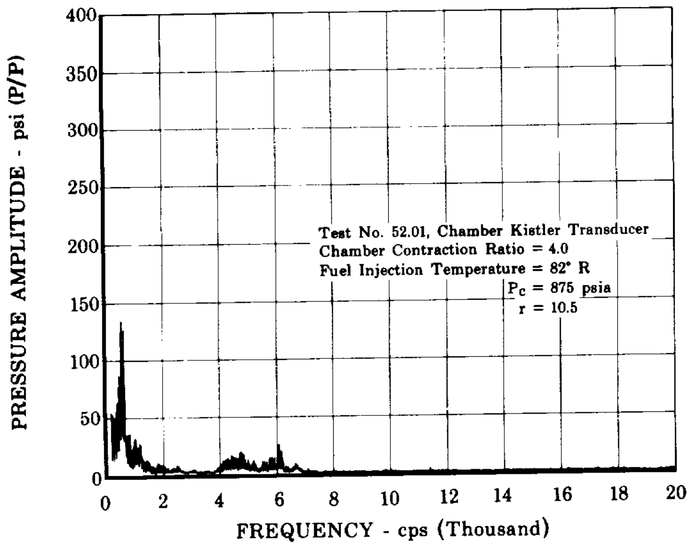

Figure III-6. Pressure Amplitude vs Frequency, Test No. 52.01, Chamber Kistler Transducer

FD 11607

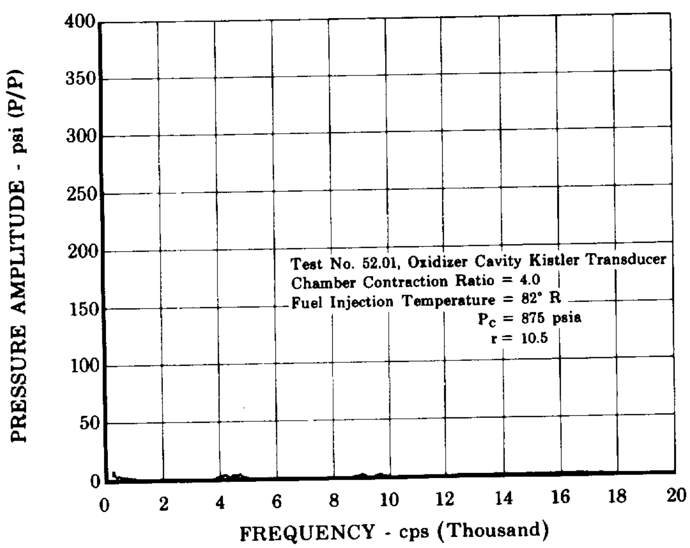

Figure III-7. Pressure Amplitude vs Frequency, Test No. 52.01, Oxidizer Cavity Kistler Transducer

FD 11606

2. Injector Configuration A4 Tests (Contraction Ratio 1.5:1)

Five test firings were conducted with injector configuration A4 at 500 psia nominal chamber pressure using the 1.5 to 1 contraction ratio nozzle. (Injector has a fuel annulus 0.182-in. ID and 0.238-in. OD, and an 0.062-in. oxidizer orifice diameter.) Full chamber-pressure test duration was reduced to 1.0 sec for these tests and the remainder of the program to minimize hardware damage. Condensed oscillograph transcriptions of chamber Kistler transducer data are presented in figure III-8 for tests 54.01, 55.01, 56.01 and 57.01.

FD 11648

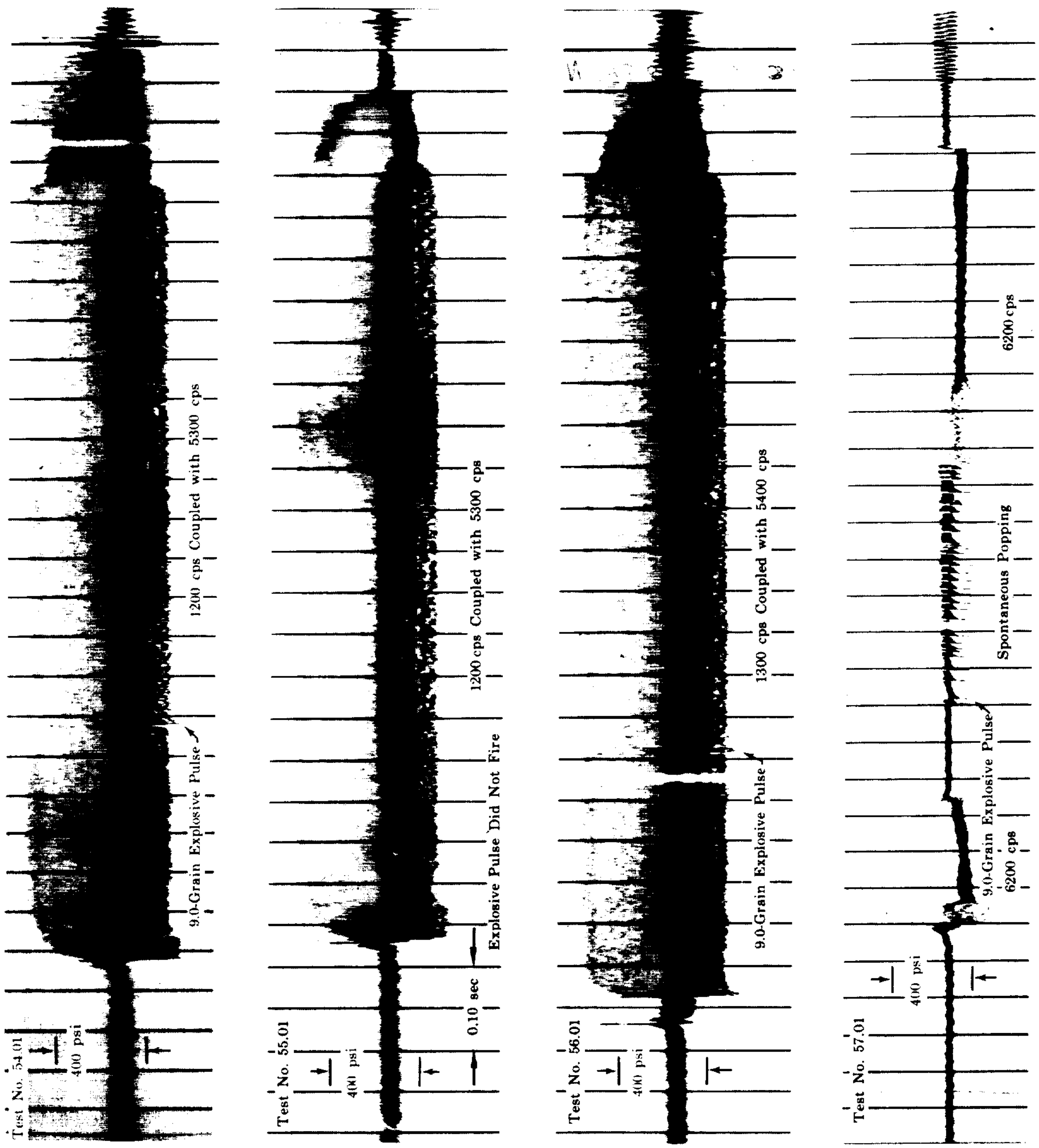

Figure III-8. Kistler Transducer Data from Tests No. 54.01, 55.01, 56.01, and 57.01

No valid chamber Kistler transducer tape data were obtained for test No. 53.04, which was conducted at 60°R fuel injection temperature. However, data were obtained from the oxidizer cavity Kistler transducer, which indicated that high-frequency combustion instability commenced at the start of the test and continued until shutdown. Figure III-9 is a pressure amplitude vs frequency distribution plot of the oxidizer cavity Kistler transducer data that indicates the existence of multiple high-frequency amplitude peaks.

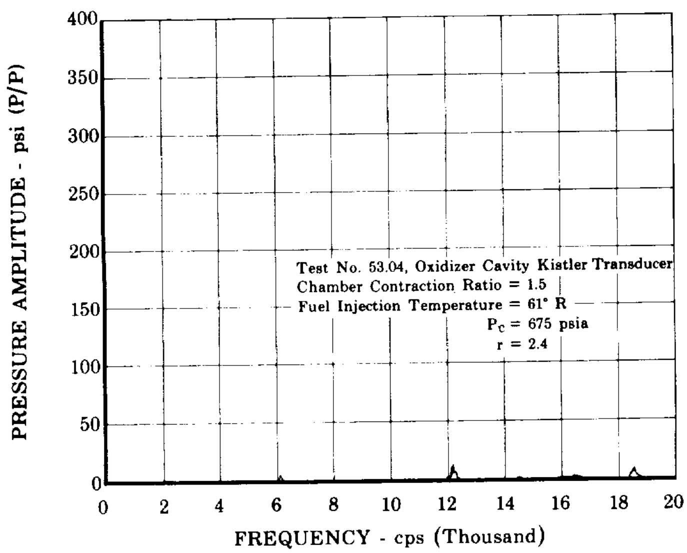

Figure III-9. Pressure Amplitude vs Frequency, Test No. 53.04, Oxidizer Cavity Kistler Transducer

FD 11609

Tests No. 54.01, 55.01, and 56.01 were conducted at approximately the same mixture ratio (4.5 to 4.8) and the same fuel injection temperature (63° to 64°R). In each test high-frequency combustion instability continued throughout the test from the start-transient. An expanded oscillograph trace (figure III-10) shows Kistler transducer data from test No. 54.01. This trace shows the explosive pulse occuring during 1200 cps coupled with 5300 cps combustion instability. This wave form is also typical for tests No. 55.01 and 56.01. Comparing the chamber and oxidizer cavity Kistler transducer amplitudes in figure III-10 indicates negligible coupling between the two. The chamber Kistler transducer pressure amplitude vs frequency distribution plot (figure III-11) indicates maximum peak-to-peak pressure amplitudes occurring at approximately 1200 cps and 5300 cps. The similarity between the pressure amplitude vs frequency distribution plot for test No. 54.01 (figure III-12) and the plot for test No. 53.04 (figure III-9) substantiates that test results were essentially the same.

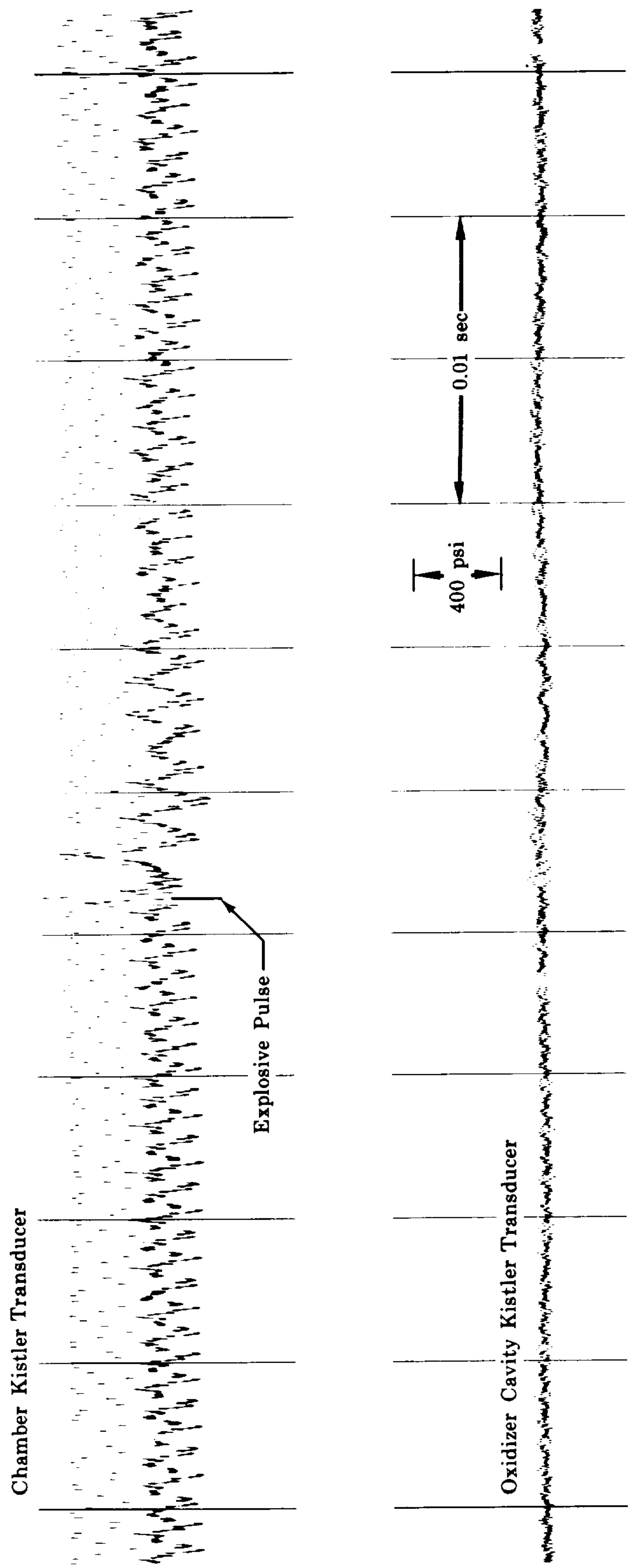

FD 11617

Figure III-10. Kistler Transducer Data from Test No. 54.01 with Explosive Pulse Occurring During 1200 cps with 5300 cps Combustion Instability

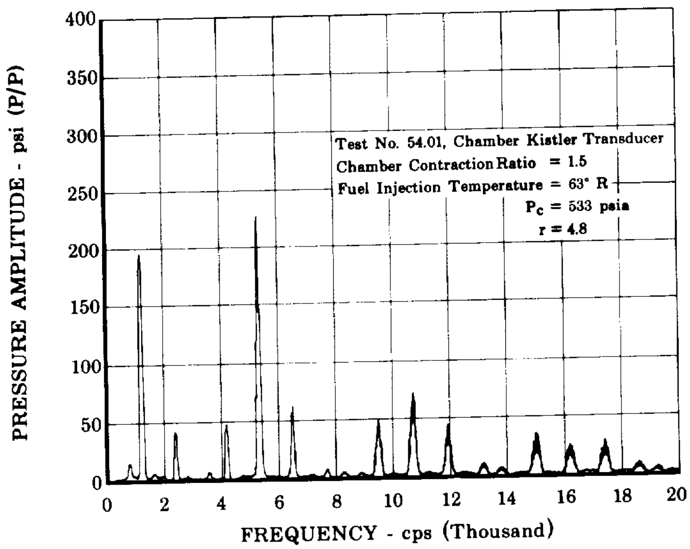

Figure III-11. Pressure Amplitude vs Frequency, Test No. 54.01, Chamber Kistler Transducer

FD 11615

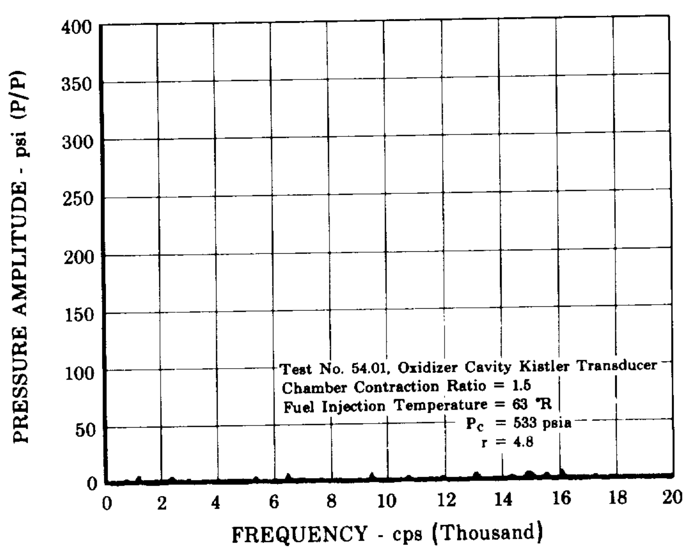

Figure III-12. Pressure Amplitude vs Frequency, Test No. 54.01, Oxidizer Cavity Kistler Transducer

FD 11614

During test No. 57.01, use of the gaseous-liquid hydrogen mixer gave a fuel injection temperature transient that varied from liquid conditions at start to a high of 178°R and back to 85°R at shutdown. Combustion instability occurred spontaneously at the test start and continued until the fuel injection temperature had increased to approximately 105°R. After the temperature had reached a maximum of 178°R and was decreasing, spontaneous popping and rough combustion began and continued for 0.3 sec until the fuel injection temperature had dropped to approximately 105°R, at which point high-frequency combustion instability resumed until shutdown. The explosive pulse unit fired soon after the start of rough combustion, however, it had no apparent effect on the combustion process. The expanded oscillograph trace (figure III-13) shows the detailed wave form as popping and rough combustion develop into sustained combustion instability. Two data points are tabulated for this test in table III-1; one during the stable period and the other after combustion instability had resumed. A pressure amplitude vs frequency distribution plot made after combustion instability had resumed (figure III-14) indicates maximum peak-to-peak pressure amplitudes occurring at approximately 6200 cps.

Values of mixture ratio and injection momentum ratio calculated for the stable combustion part of the test were based on an assumed combustion efficiency and measured values of chamber pressure and oxidizer flow. This technique was used because the fuel flow meter and temperature instrumentation transient response, when gas is introduced into the system, may not be indicative of the instantaneous true injection conditions.

3. Injector Configuration C1 Tests (Contraction Ratio 1.5:1)

Six test firings were conducted with injector configuration C1 at 500 psia nominal chamber pressure using the 1.5 to 1 contraction ratio nozzle. (Injector has a fuel orifice annulus 0.182-in. ID and 0.194-in. OD, and an 0.099-in. oxidizer orifice diameter.) Condensed oscillograph transcriptions of chamber Kistler transducer data are presented in figures III-15 and III-16 for tests No. 58.04, 59.01, 60.01, 61.01, 62.01, and 63.01.

Test No. 58.04 was conducted at 61°R fuel injection temperature. The test began with well developed chugging that was attributed to low oxidizer injection pressure drop. The 9.0-grain explosive pulse fired satisfactorily; however, its perturbation was quickly damped. The 14.4-grain explosive pulse triggered sustained high-frequency combustion instability, which continued until shutdown. The expanded oscillograph trace (figure III-17) shows the chugging frequency triggered into high-frequency combustion instability. The pressure amplitude vs frequency distribution plot (figure III-18) shows three predominant peak-to-peak pressure amplitudes occurring at approximately 6100 cps, 12,300 cps, and 18,600 cps.

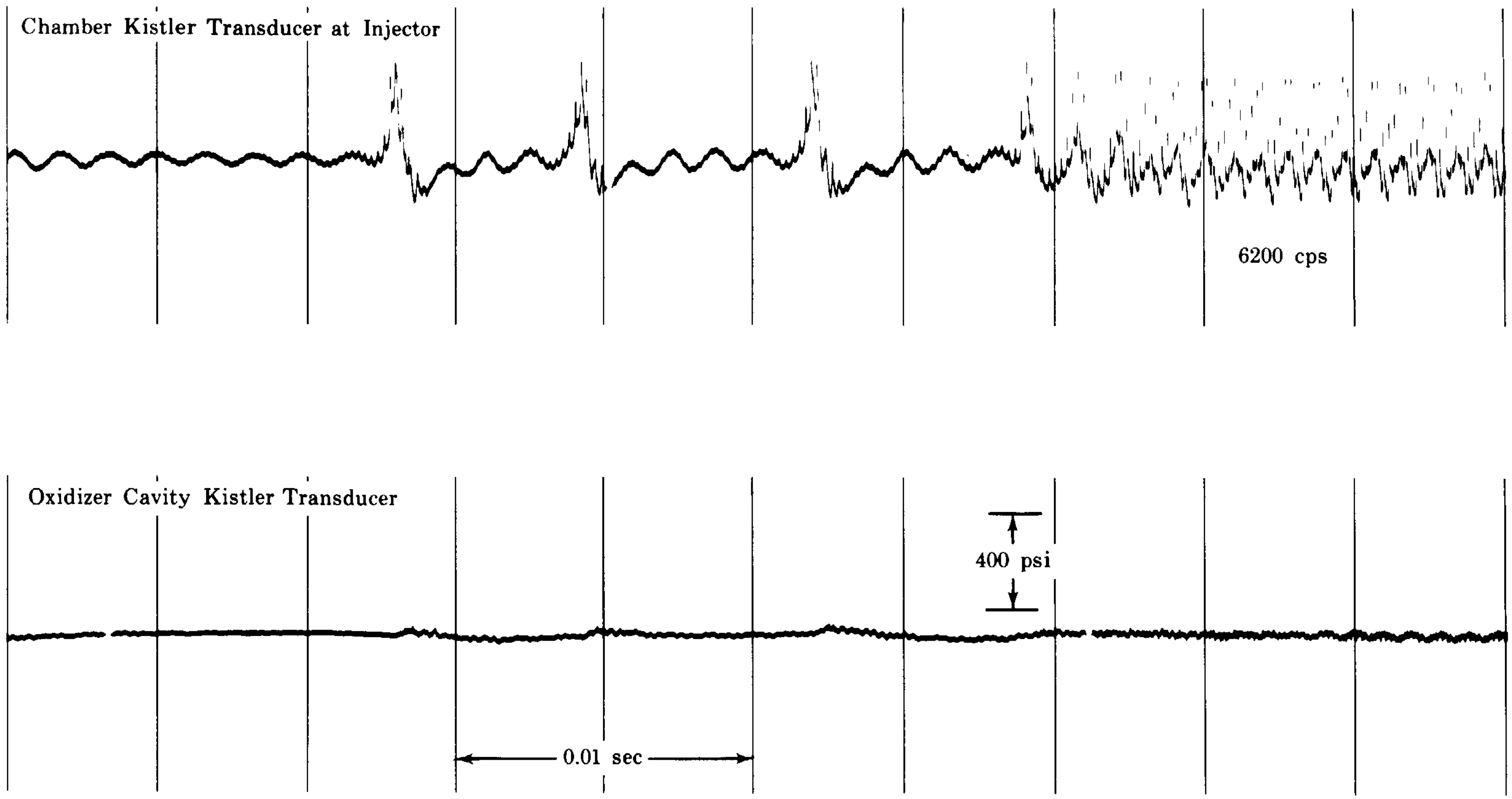

Figure III-13. Transducer Data from Test No. 57.01 Showing Detail Wave Form as Popping and Rough Combustion Developing into Sustained Combustion Instability

FD 11654

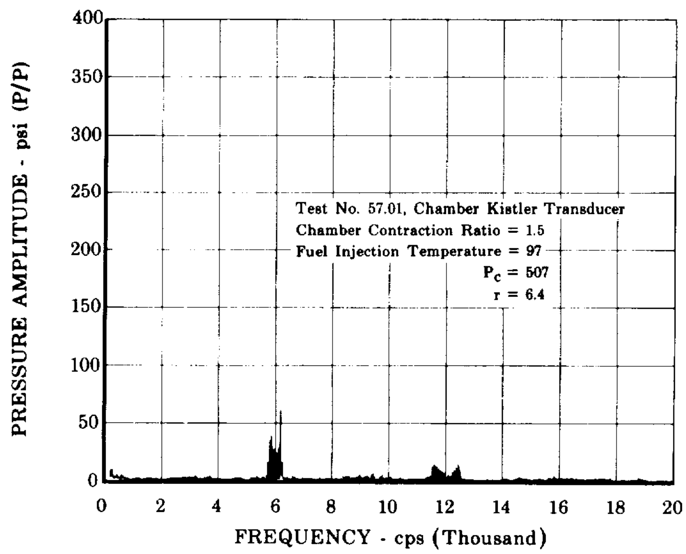

Figure III-14. Pressure Amplitude vs Frequency, Test No. 57.01, Chamber Kistler Transducer — FD 11612

FD 11643

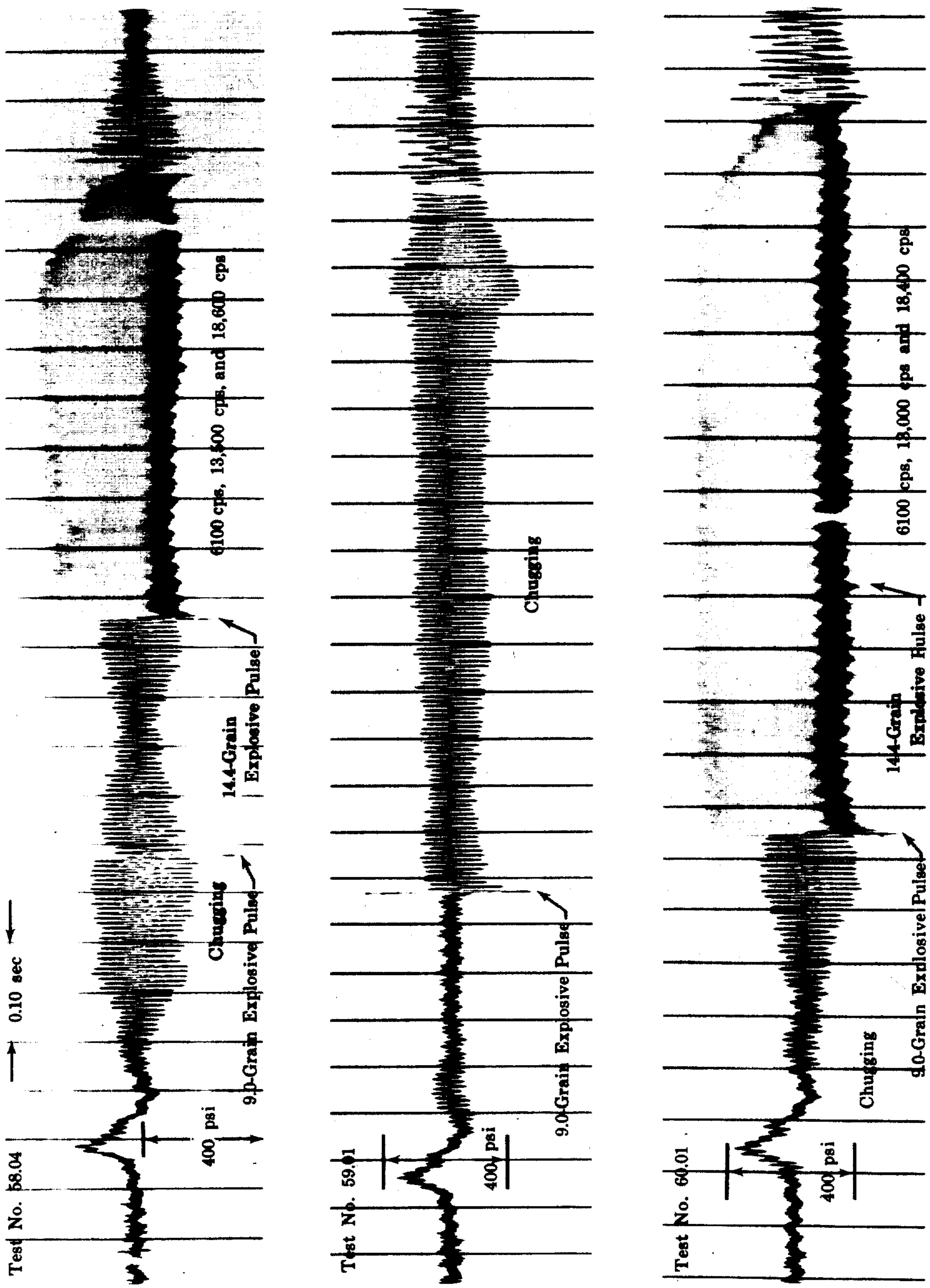

Figure III-15. Kistler Transducer Data from Tests No. 58.04, 59.01, and 60.01

FD 11647

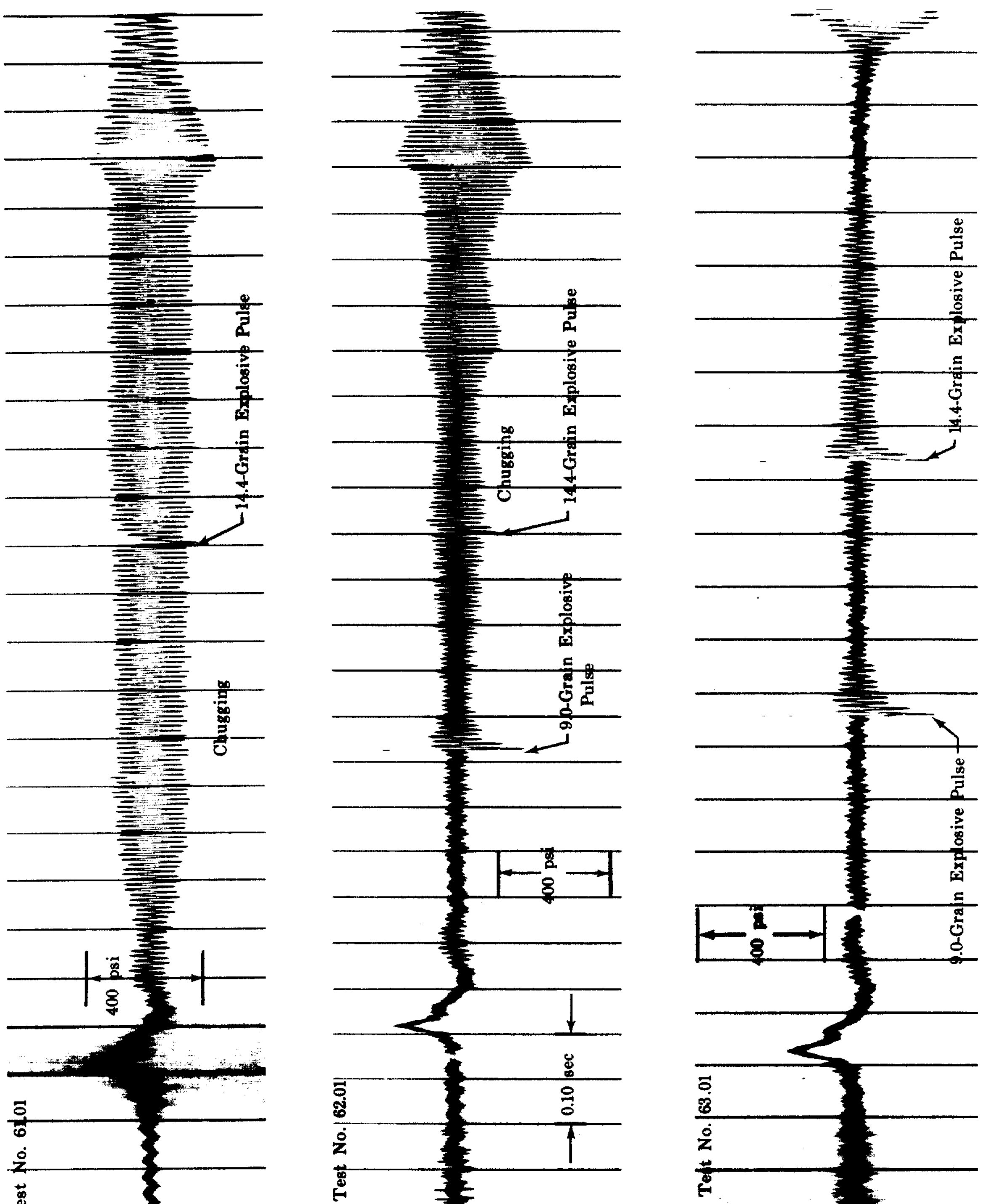

Figure III-16. Kistler Transducer Data from Tests No. 61.01, 62.01, and 63.01

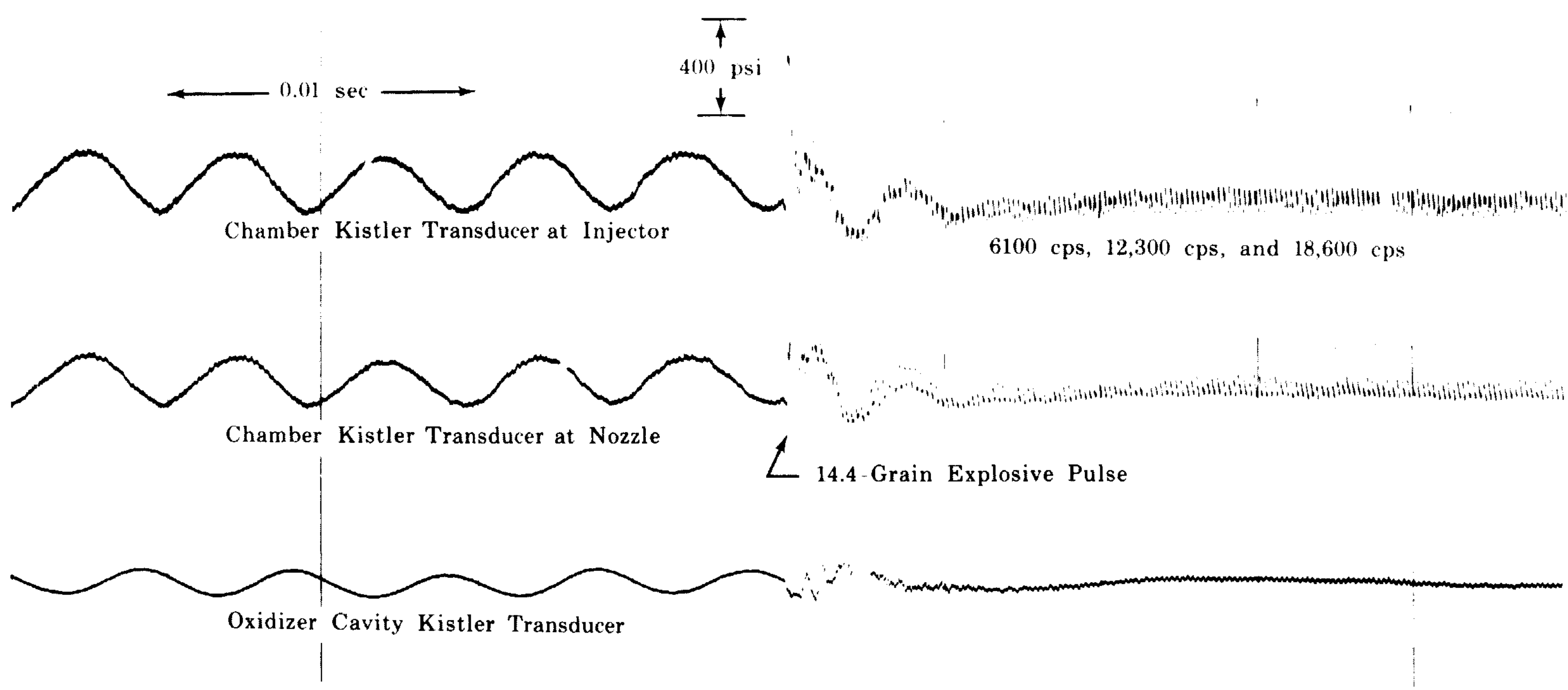

Figure III-17. Transducer Data from Test No. 58.04 Showing Chugging Triggered into High-Frequency Combustion Instability by 14.4-Grain Explosive Pulse

FD 11649

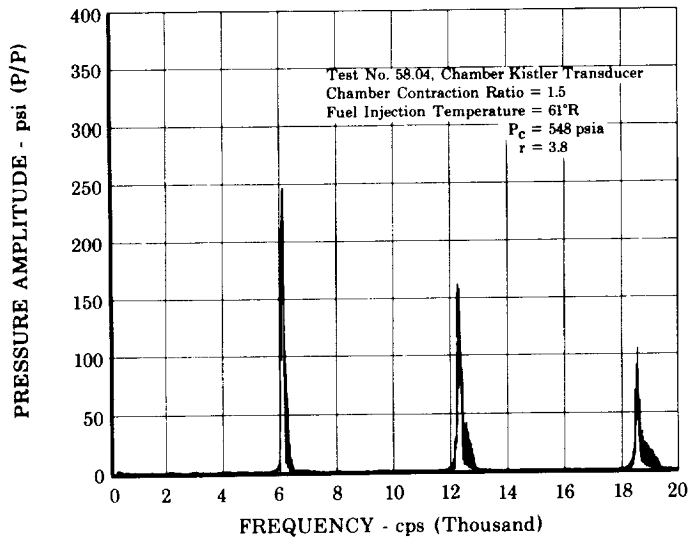

Figure III-18. Pressure Amplitude vs Frequency, Test No. 58.04, Chamber Kistler Transducer FD 11598

Test No. 59.01 was conducted at 62°R fuel injection temperature. The test began with sustained chugging that continued until shutdown. Both explosive pulses fired satisfactorily, however, neither triggered high-frequency combustion instability.

Test No. 60.01, conducted at 62°R fuel injection temperature, was similar to test No. 58.04. The test began with well developed chugging that was triggered into high-frequency combustion instability by the 9.0-grain explosive pulse. The 14.4-grain explosive pulse fired, but did not affect the high-frequency combustion instability. A pressure amplitude vs frequency distribution plot made after high-frequency combustion instability had been triggered (figure III-19) shows maximum peak-to-peak pressure amplitudes occurring at approximately 6100 cps, 12,300 cps, and 18,500 cps.

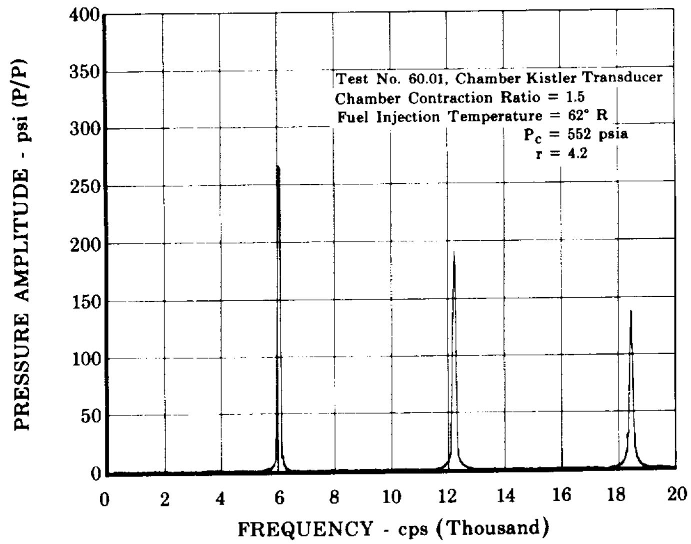

Figure III-19. Pressure Amplitude vs Frequency, Test No. 60.01, Chamber Kistler Transducer FD 11596

The gaseous-liquid hydrogen mixer was used during tests No. 61.01 and 62.01 to provide fuel injection temperatures of 87°and 88°R. Test No. 61.01 began with well developed chugging that continued until shutdown. Only the second explosive pulse fired; however, it did not trigger high-frequency combustion instability. Test No. 62.01 began with stable combustion. The 9.0-grain explosive pulse triggered chugging that continued until shutdown. The 14.4-grain explosive pulse fired satisfactorily but its perturbation was quickly damped. The pressure amplitude vs frequency distribution plot for test No. 61.01 (figure III-20) is typical for the chugging type of combustion experienced during this test series. The pressure amplitude vs frequency distribution plot of data from the Kistler transducer located in the oxidizer cavity (figure III-21) is typical of the 180° out of phase coupling with chamber pressure oscillations experienced during chugging.

Test No. 63.01 was conducted at 61°R fuel injection temperature. This test was similar in temperature to test No. 58.04; however, it began with fairly stable combustion. Both explosive pulses fired but only triggered chugging that tended to damp out.

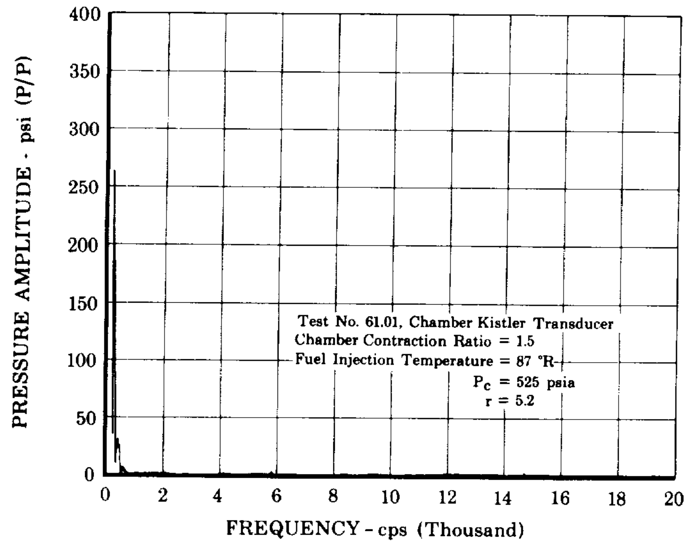

Figure III-20. Pressure Amplitude vs Frequency, Test No. 61.01, Chamber Kistler Transducer — FD 11601

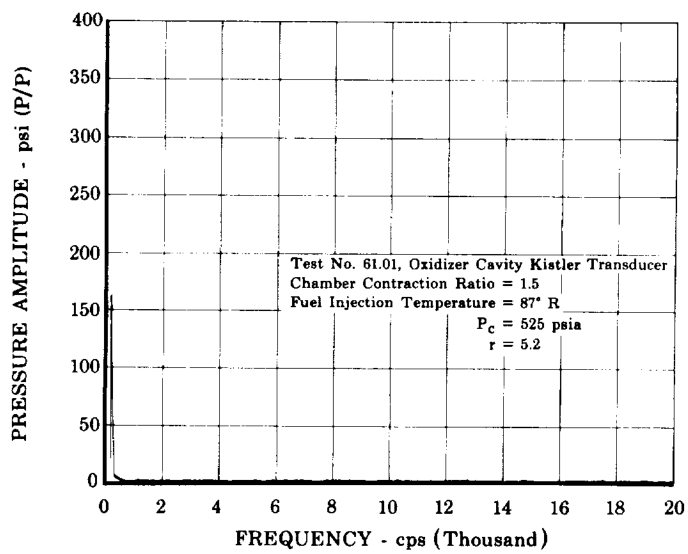

Figure III-21. Pressure Amplitude vs Frequency, Test No. 61.01, Oxidizer Cavity Kistler Transducer — FD 11602

4. Injector Configuration A4 Tests (Contraction Ratio 2.5:1)

Three test firings were conducted with injector configuration A4 at a 500 psia nominal chamber pressure using the 2.5 to 1 contraction ratio nozzle. Condensed oscillograph transcriptions of chamber Kistler transducer data are presented in figure III-22 for tests No. 64.01, 65.01, and 66.01.

FD 11681

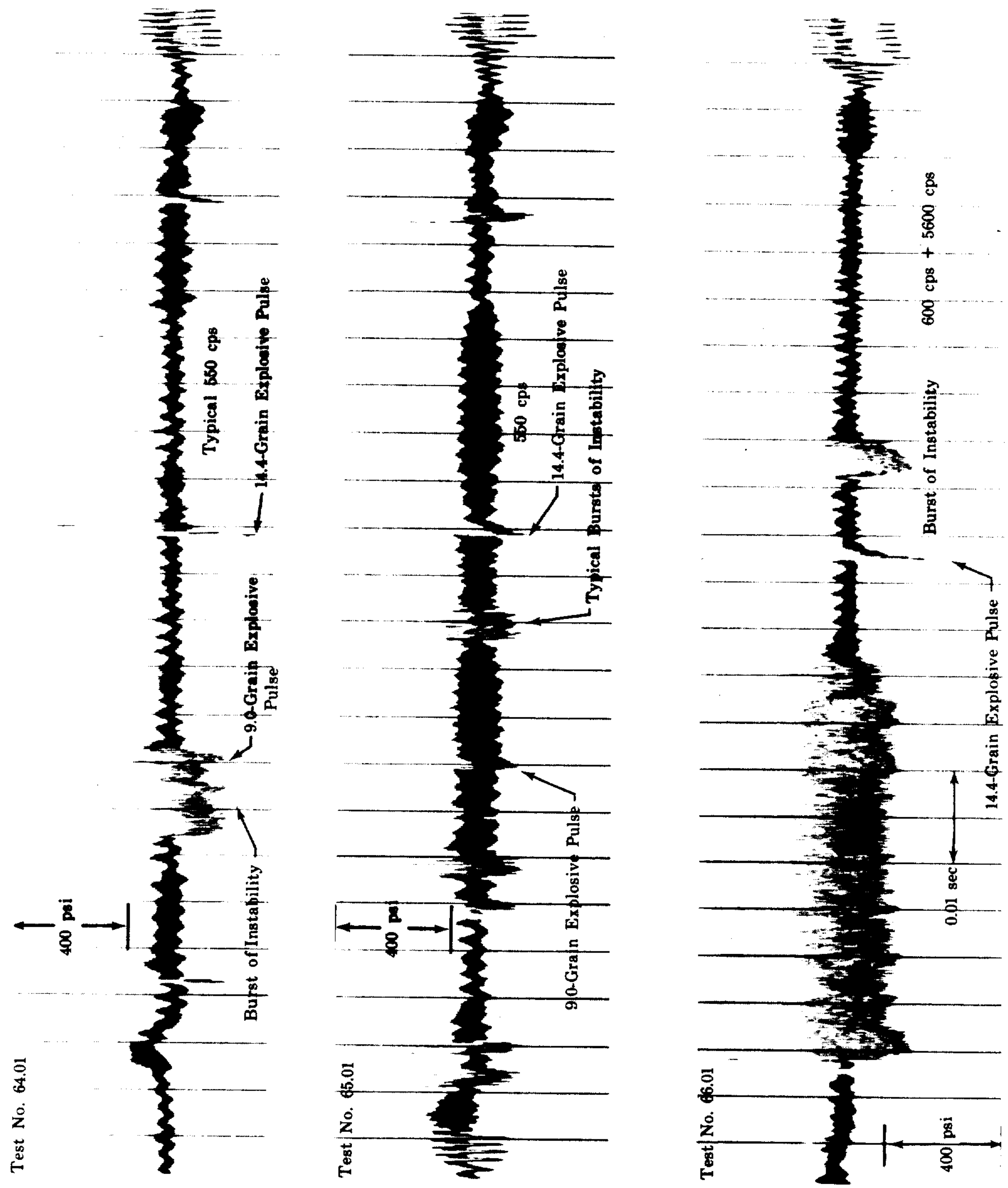

Figure III-22. Kistler Transducer Data from Tests No. 64.01, 65.01, and 66.01

Test No. 64.01 was conducted at 69°R fuel injection temperature. The test started with sustained (approximately 550 cps) intermediate-frequency combustion instability, which spontaneously burst into high-frequency combined with intermediate-frequency combustion instability. The 9.0-grain explosive pulse stopped the high-frequency instability; however, the 550 cps intermediate-frequency instability continued until shutdown. The 14.4-grain explosive pulse fired satisfactorily but its perturbation was quickly damped. Two data points are tabulated for this test in table III-1; one during high-frequency combined with intermediate-frequency combustion instability, and the other after the high-frequency instability had been stopped by the explosive pulse. The expanded oscillograph trace (figure III-23) shows high-frequency coupled with intermediate-frequency combustion instability and the 9.0-grain explosive pulse damping out only the high-frequency portion of the instability.

Test No. 65.01 was conducted with 72°R fuel injection temperature. The test began with sustained (approximately 550 cps) intermediate-frequency combustion instability, which persisted until shutdown. Two short bursts of high-frequency coupled with the intermediate-frequency combustion instability occurred prior to the first explosive pulse. An expanded oscillograph trace of a third burst of high-frequency instability occurring between the first and second explosive pulses is shown in figure III-24.

Test No. 66.01 was conducted at 65°R fuel injection temperature. The test began with high-frequency coupled with intermediate-frequency (approximately 600 cps) combustion instability. The high-frequency instability portion damped prior to the second explosive pulse, however, the intermediate-frequency continued until shutdown. The first explosive pulse did not operate. A short burst of high-frequency coupled with the intermediate-frequency instability occurred 80 ms after the second pulse had fired. An expanded oscillograph trace of the diminishing amplitude high-frequency portion of the high-frequency coupled with intermediate-frequency combustion instability is shown in figure III-25. A pressure amplitude vs frequency distribution plot (figure III-26) made during the first part of the test shows predominant peak-to-peak pressure amplitudes occuring at approximately 600 cps and 5500 cps.

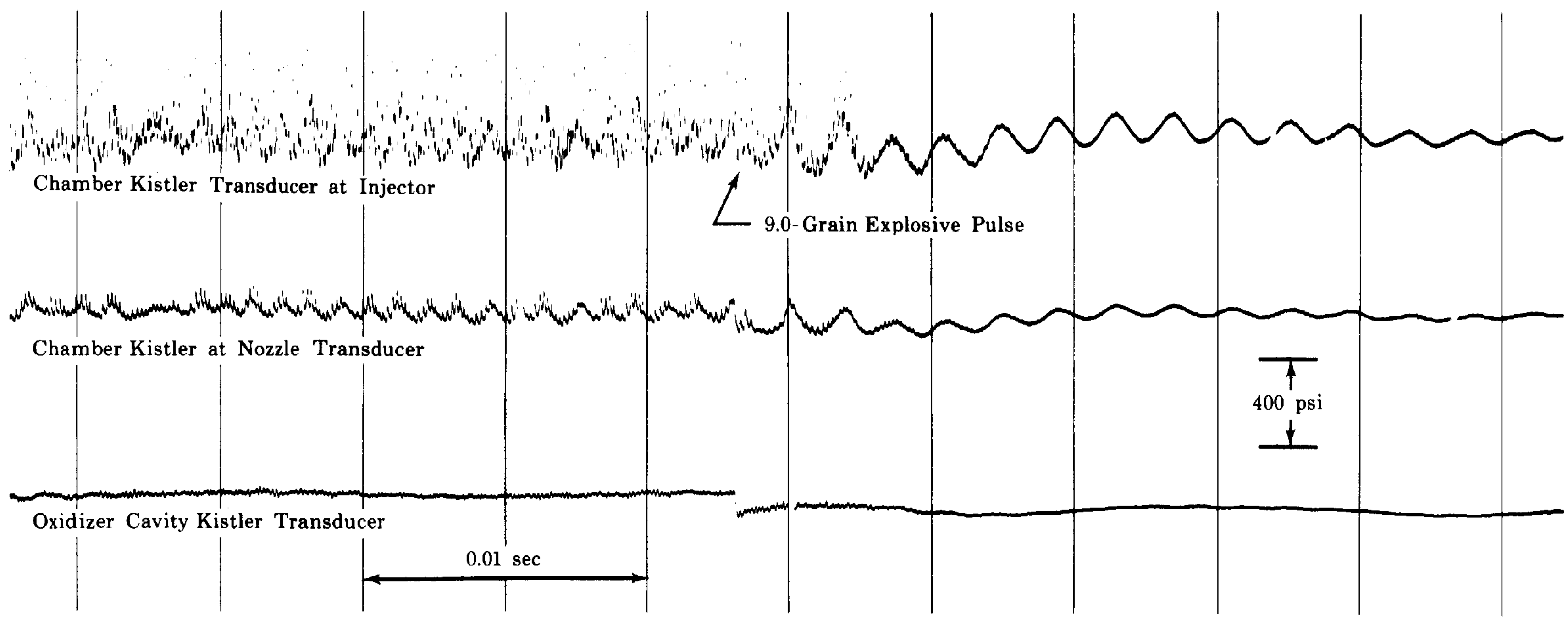

Figure III-23. Transducer Data from Test No. 64.01 Showing High-Frequency Coupled with Intermediate-Frequency Combustion Instability and the Explosive Pulse Damping only the High-Frequency Portion of the Instability

FD 11619

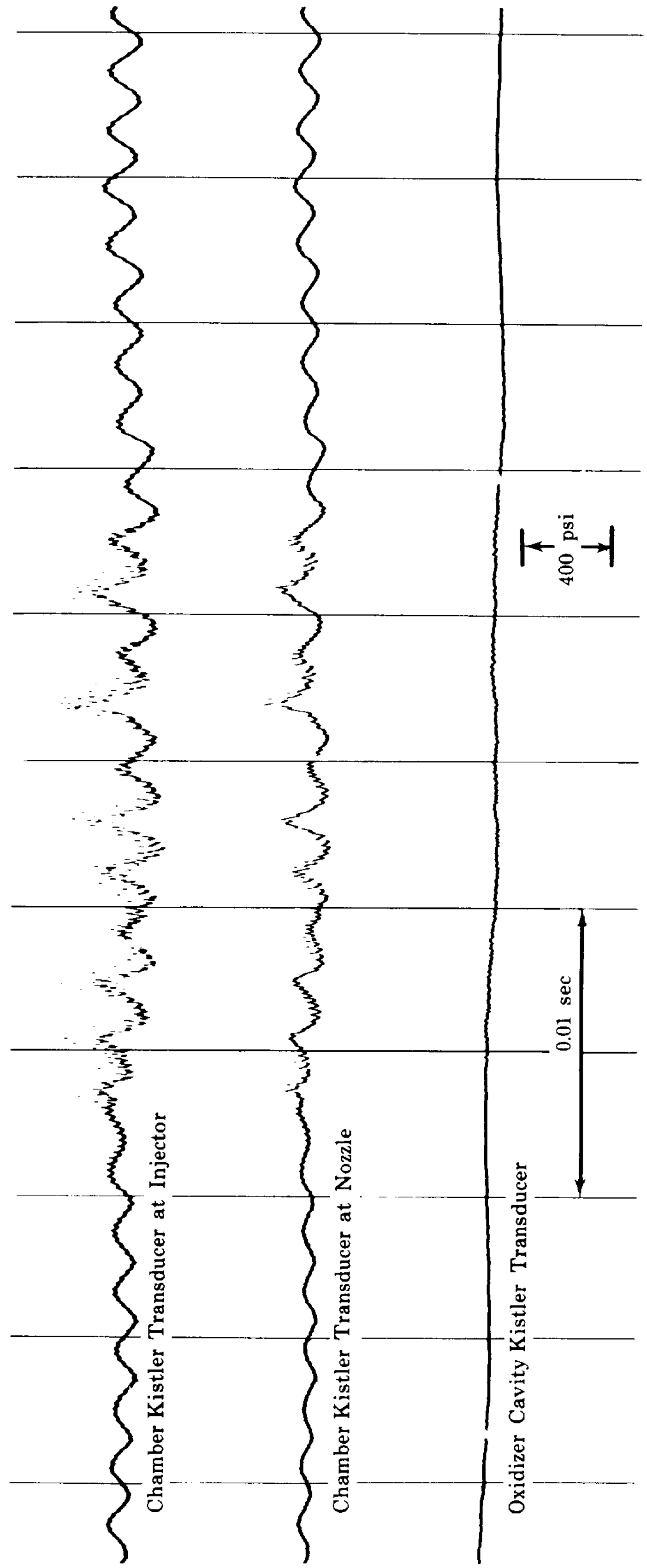

FD 11618

Figure III-24. Transducer Data from Test No. 65.01 Showing a Burst of High-Frequency Coupled with Sustained Intermediate-Frequency Combustion Instability

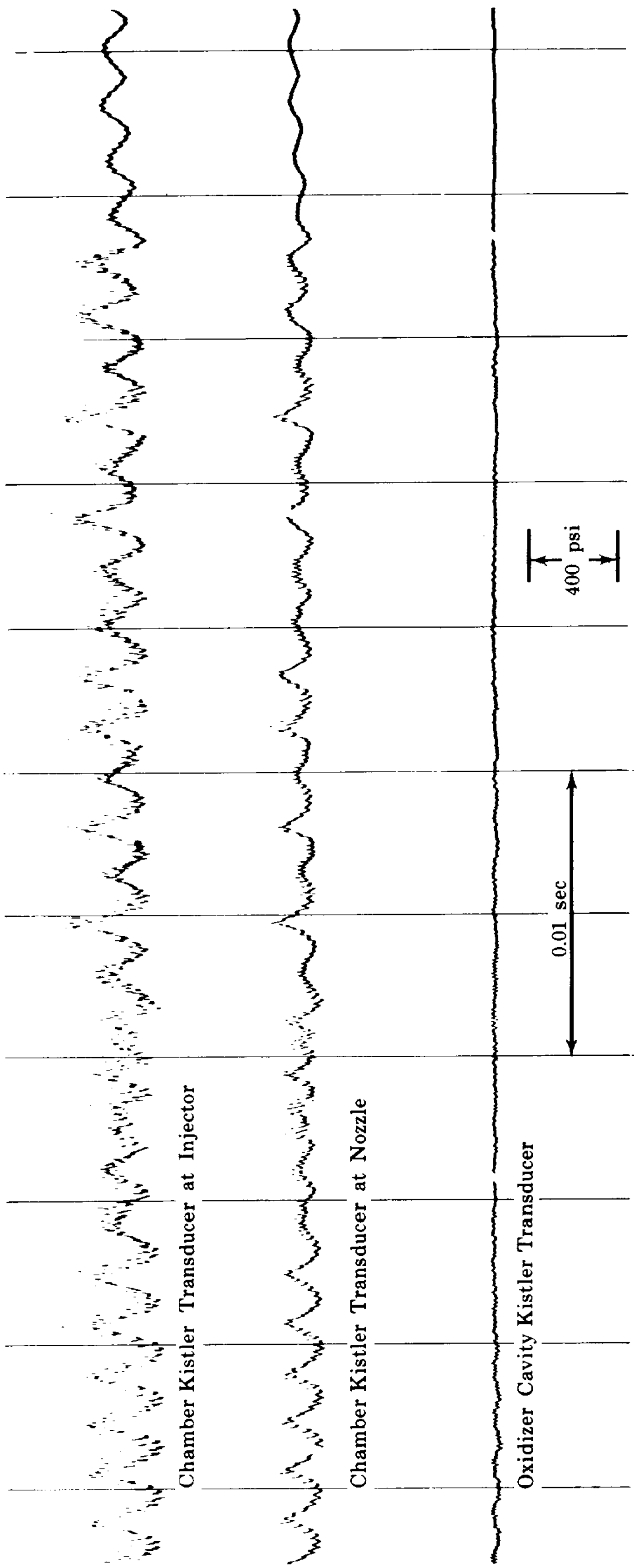

FD 11642

Figure III-25. Transducer Data from Test No. 66.01 Showing the High-Frequency Portion of the High-Frequency Coupled with Intermediate-Frequency Combustion Instabilty Damping

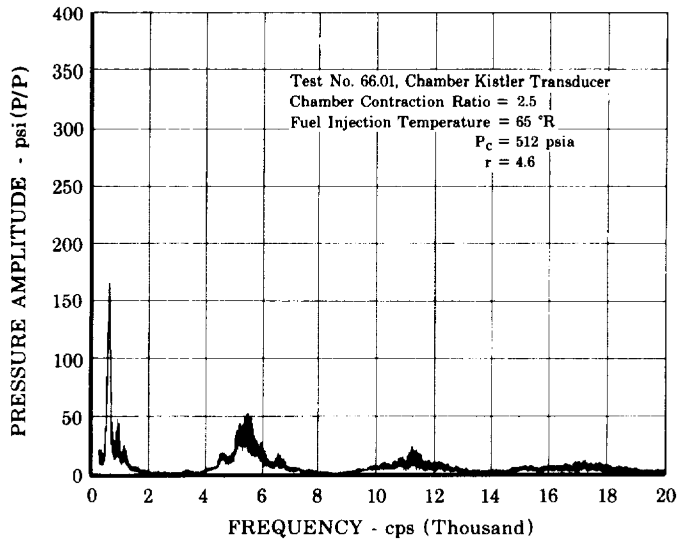

Figure III-26. Pressure Amplitude vs Frequency, Test No. 66.01, Chamber Kistler Transducer FD 11599

5. Injector Configuration D2 Tests (Contraction Ratio 2.5:1)

Two test firings were conducted with injector configuration D2 at 900 psia nominal chamber pressure using the 2.5 to 1 contraction ratio nozzle. (Injector has a fuel orifice annulus 0.182-in. ID and 0.201-in. OD, and an 0.133-in. oxidizer orifice diameter.) Condensed oscillograph transcriptions of chamber Kistler transducer data are presented in figure III-27 for tests No. 67.01 and 68.01.

Test No. 67.01 was conducted at 59°R fuel injection temperature. The test began with severe sustained chugging that continued until shutdown. The 9.0-grain explosive pulse fired but was quickly damped. The 14.4-grain explosive pulse did not operate. The chugging was attributed to an oxidizer injector low pressure drop configuration that was used to obtain a high injection momentum ratio.

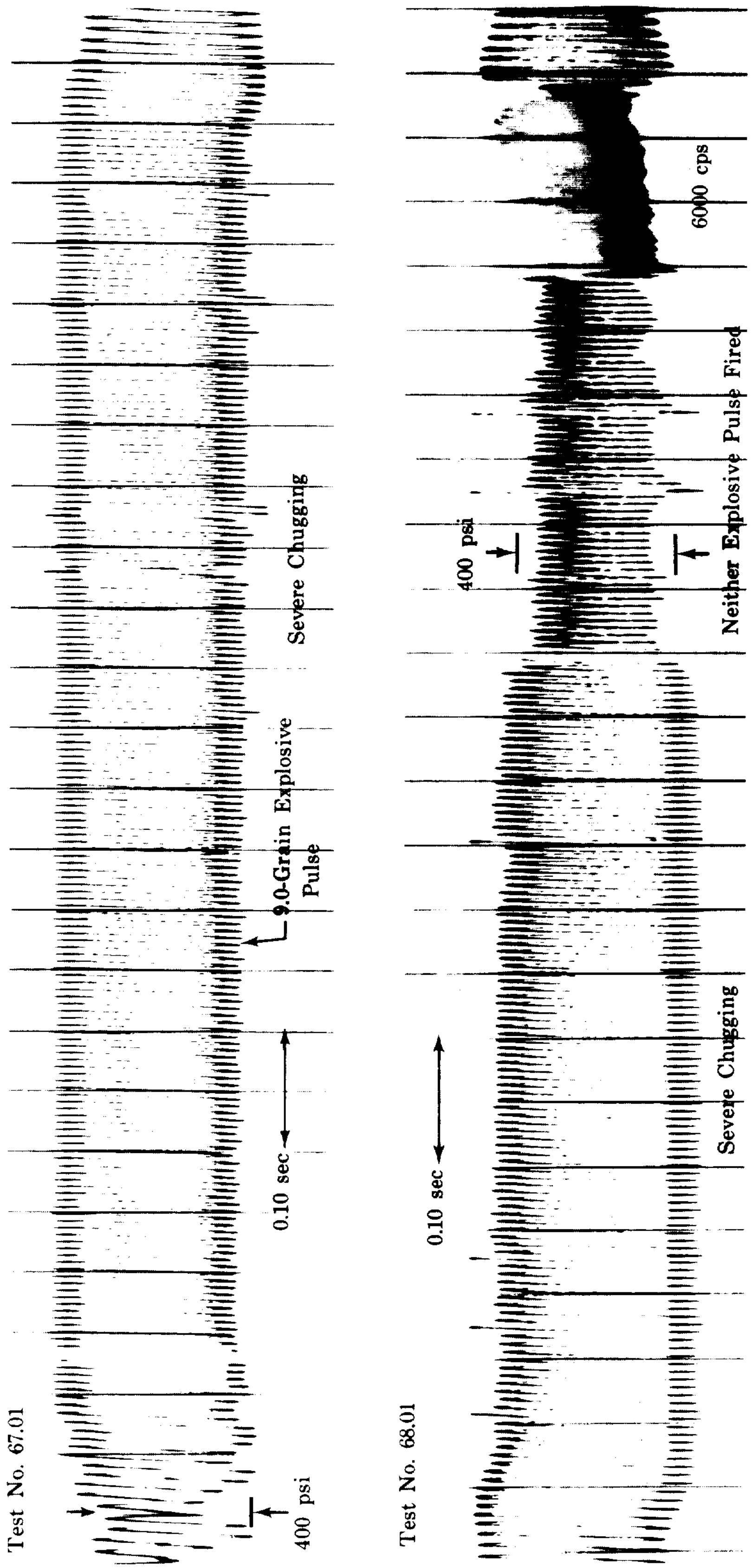

FD 11645

Figure III-27. Kistler Transducer Data from Tests No. 67.01 and 68.01

Test No. 68.01 was conducted at approximately the same fuel injection temperature as test No. 67.01 and it also started with severe sustained chugging. During this test neither of the explosive pulse units operated. Some erosion of the nozzle throat occurred and as the effective contraction ratio decreased, high-frequency combustion instability began spontaneously near the test completion. Two data points are presented for this test in table III-1; one during the chugging period and the other after high-frequency combustion instability had commenced. An expanded oscillograph trace of chugging and the spontaneous occurrence of high-frequency combustion instability is shown in figure III-28. This was the first time that high-frequency oscillations (approximately 12,000 cps) with amplitudes approaching those of chamber oscillations, had occurred in the oxidizer cavity. A pressure amplitude vs frequency distribution plot of chamber Kistler transducer data made after high-frequency instability had begun, indicates a predominant peak-to-peak pressure amplitude occurring at approximately 6000 cps. (See figure III-29.)

Because erosion of the nozzle throat occurred during this test, an effective contraction ratio was calculated. This calculation was based on an assumed combustion efficiency and measured values of chamber pressure and total propellant flow. A contraction ratio of approximately 1.75 to 1 was calculated for the moment when high-frequency combustion instability commenced.

6. Injector Configuration A4 Tests (Contraction Ratio 4.0:1)

Four test firings were conducted with injector configuration A4 at 500 psia nominal chamber pressure using the 4.0 to 1 contraction ratio nozzle. Condensed oscillograph transcriptions of chamber Kistler transducer data are presented in figure III-30 for tests No. 69.05, 70.02, 71.03, and 72.01.

Test No. 69.05 was conducted at 69°R fuel injection temperature. The test began with sustained 600 cps intermediate-frequency combustion instability that persisted until shutdown. Both explosive pulses fired but were quickly damped.

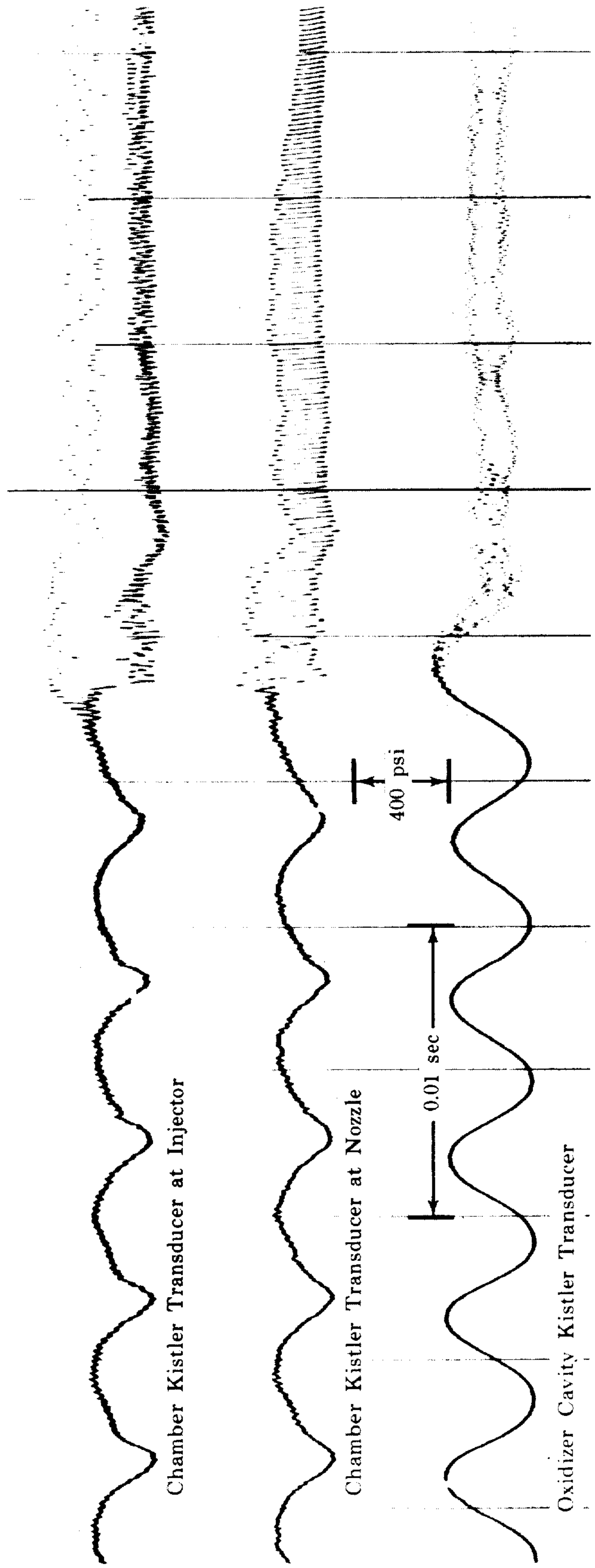

FD 11682

Figure III-28. Transducer Data from Test No. 68.01 Showing Chugging and the Spontaneous Occurrence of High-Frequency Combustion Instability

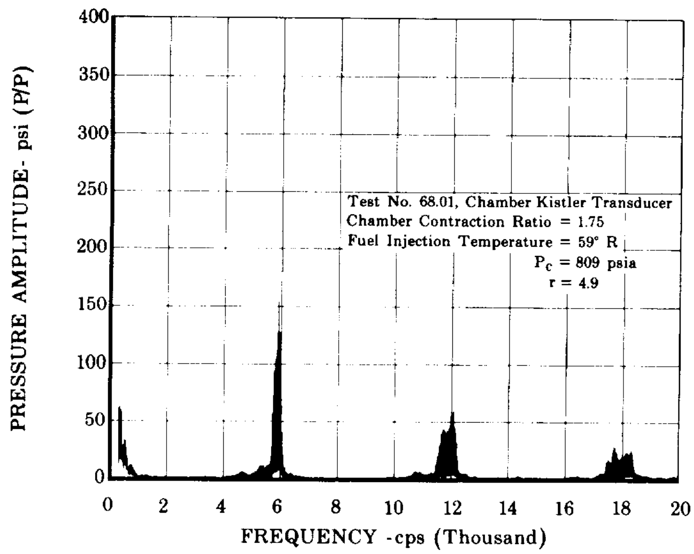

Figure III-29. Pressure Amplitude vs Frequency, Test No. 68.01, Chamber Kistler Transducer

FD 11683

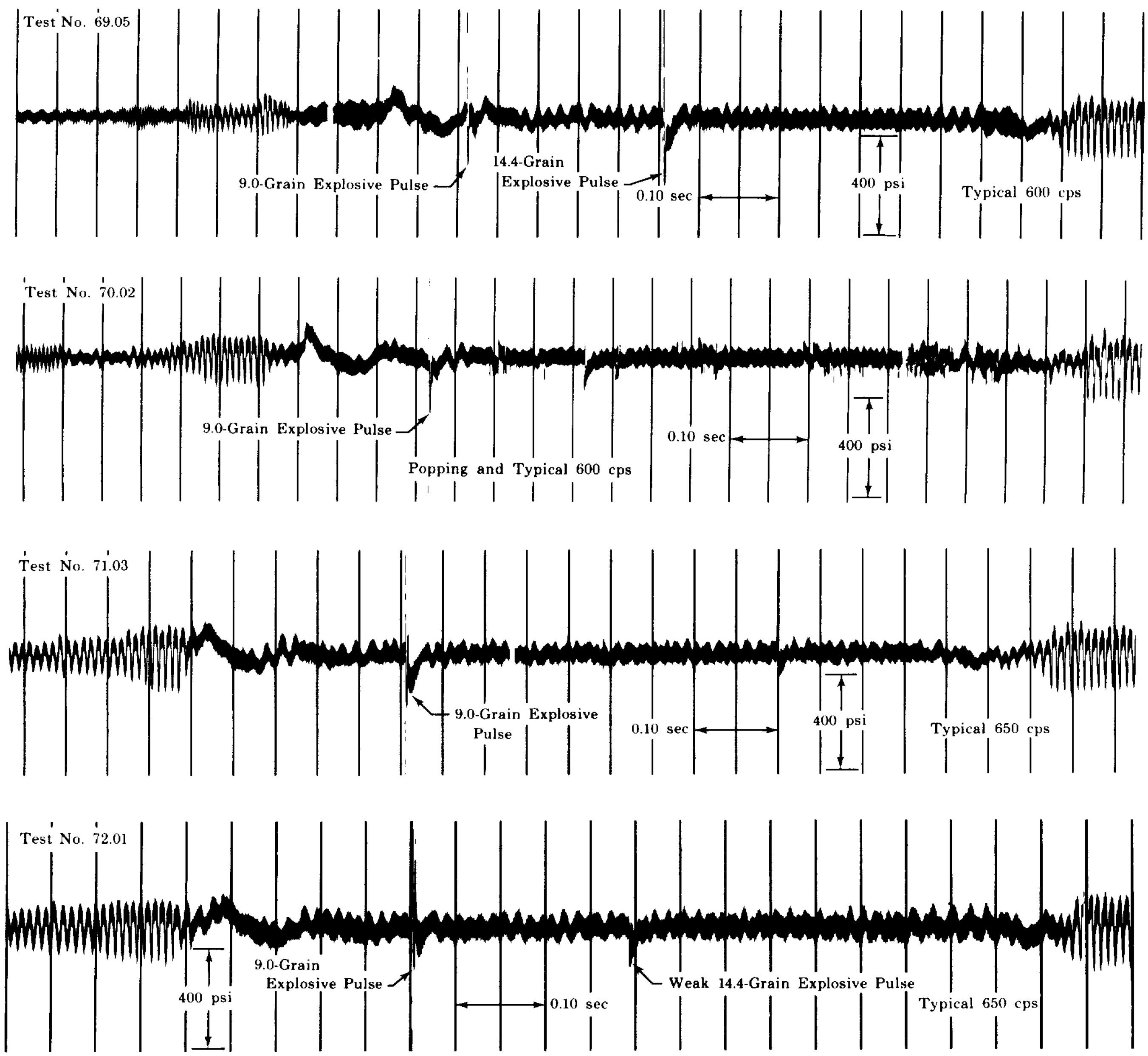

Figure III-30. Kistler Transducer Data from Tests No. 69.05, 70.02, 71.03, and 72.01 FD 11603

Test No. 70.02 was conducted at 67°R fuel injection temperature. The test began with sustained 600 cps intermediate-frequency combustion instability that continued until shutdown. Some spontaneous popping was observed. Only the 9.0-grain explosive pulse fired and was quickly damped.

Test No. 71.03 was conducted at 70°R fuel injection temperature. The test began with sustained 650 cps intermediate-frequency combustion instability that continued until shutdown. Only the 9.0-grain explosive pulse fired and was quickly damped.

Test No. 72.01 was conducted at 68°R fuel injection temperature. Similar to the previous three tests, this test also began with sustained 650 cps intermediate-frequency combustion instability that continued until shutdown. The 9.0-grain explosive pulse was quickly damped. The 14.4-grain explosive pulse fired but appeared to be weak and was also quickly damped. An expanded oscillograph trace (figure III-31) shows the typical 650 cps intermediate-frequency combustion instability and the quickly damped 9.0-grain explosive pulse. The pressure amplitude vs frequency distribution plot of test No. 72.01 presented in figure III-32 is typical for these last four test firings.

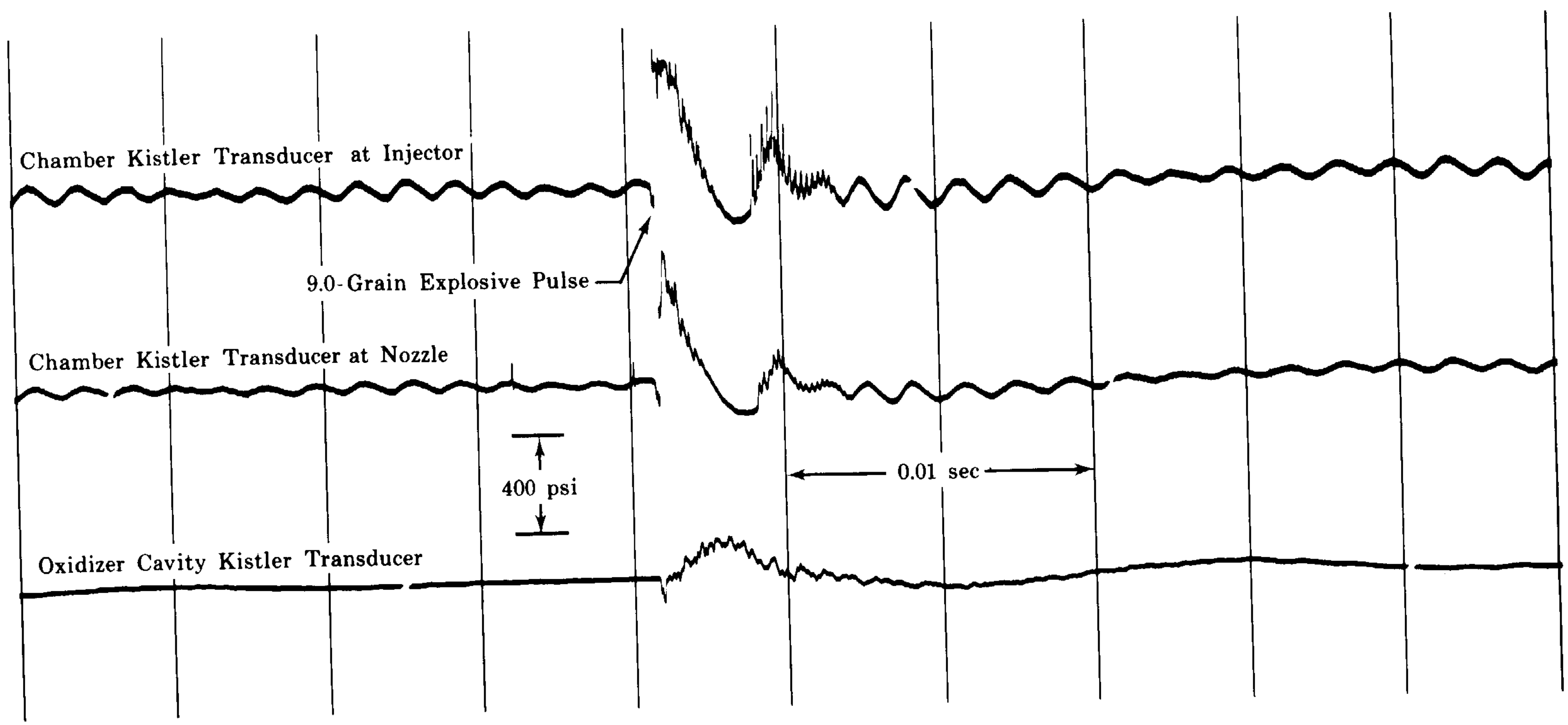

FD 11620

Figure III-31. Transducer Data from Test No. 72.01 Showing Typical 650 cps Intermediate-Frequency Combustion Instability and Quickly Damped Explosive Pulse

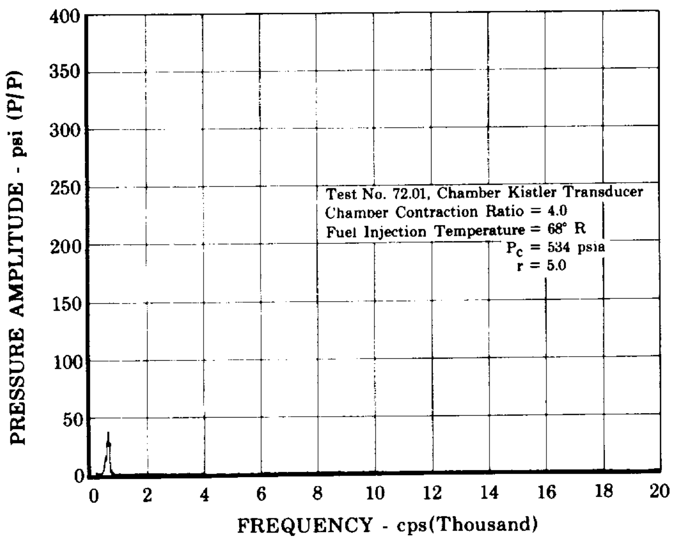

Figure III-32. Pressure Amplitude vs Frequency, Test No. 72.01, Chamber Kistler Transducer

FD 11684

SECTION IV
PRELIMINARY ANALYSIS OF RESULTS

The results of tests conducted during this report period have been added to the data correlations being maintained with Phase I and prior Phase II test data. The program variables are plotted in these correlations in an effort to separate the stable and unstable regions. A plot of injection momentum ratio vs hydrogen inlet temperature has previously provided this separation successfully. Addition of the most recent data to this correlation confirms the previously observed separation and provides a more definite indication of a chamber contraction ratio effect.

Figures IV-1, IV-2, and IV-3 present injection momentum ratio vs hydrogen inlet temperature for the three slab motor contraction ratios tested: 1.5, 2.5, and 4.0. Stable and unstable points are identified. For these plots, data points in which other effects may be present (chugging, improper pulser operation, or swirlers in the injector) have been omitted. The dashed line on each plot is a best estimate of the separation between stable and unstable regions. The presence of some stable points in the unstable region is probably the result of insufficient triggering energy being released in those particular tests or an indication of marginally stable conditions.

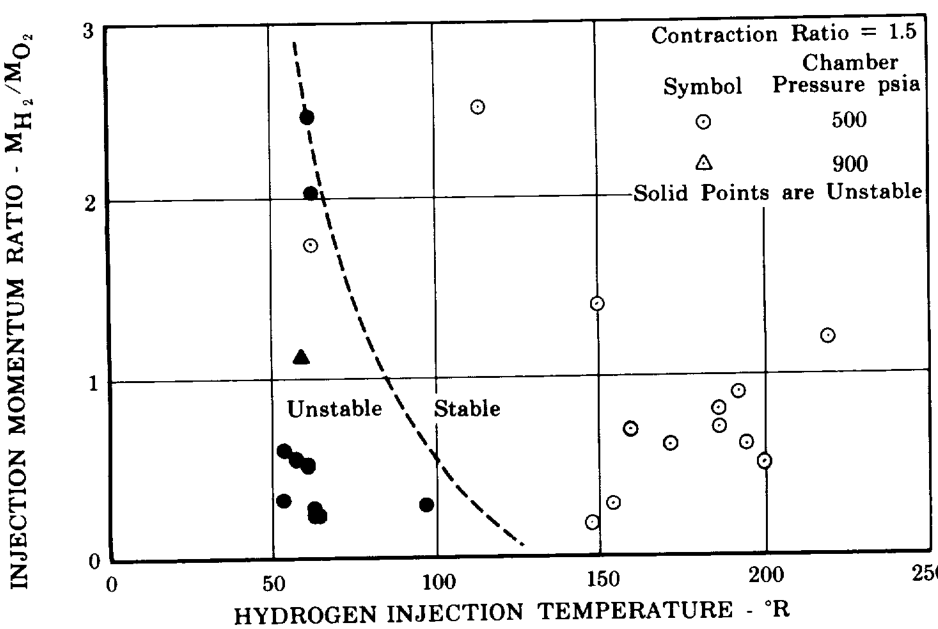

Figure IV-1. Indicated Effect of Injection Momentum Ratio and Hydrogen Temperature at a Contraction Ratio of 1.5 on Slab Motor Stability (Separated by Nominal Chamber Pressure) FD 11633

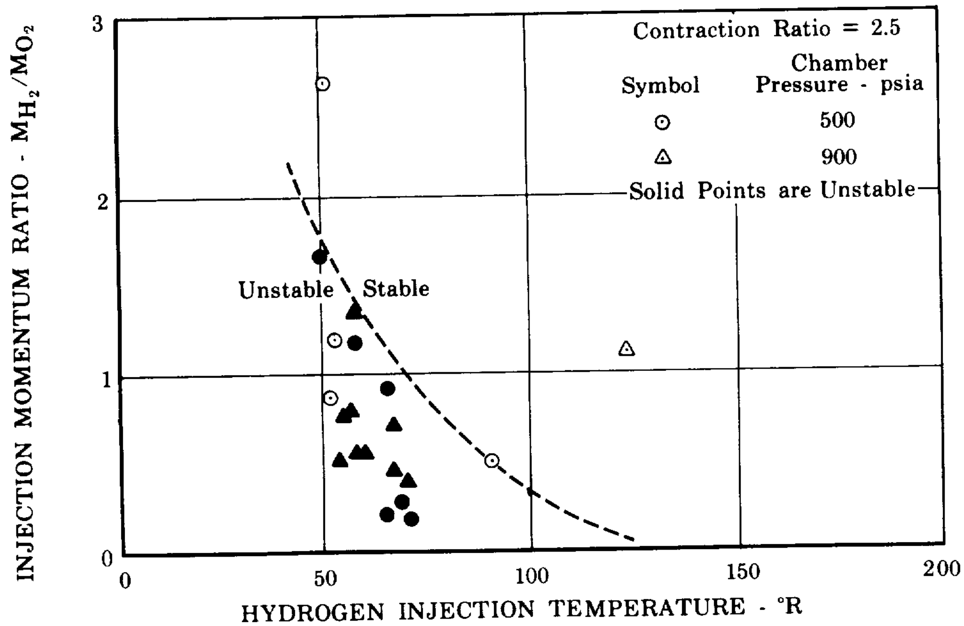

Figure IV-2. Indicated Effect of Injection Momentum Ratio and Hydrogen Temperature at a Contraction Ratio of 2.5 on Slab Motor Stability (Separated by Nominal Chamber Pressure) FD 11631

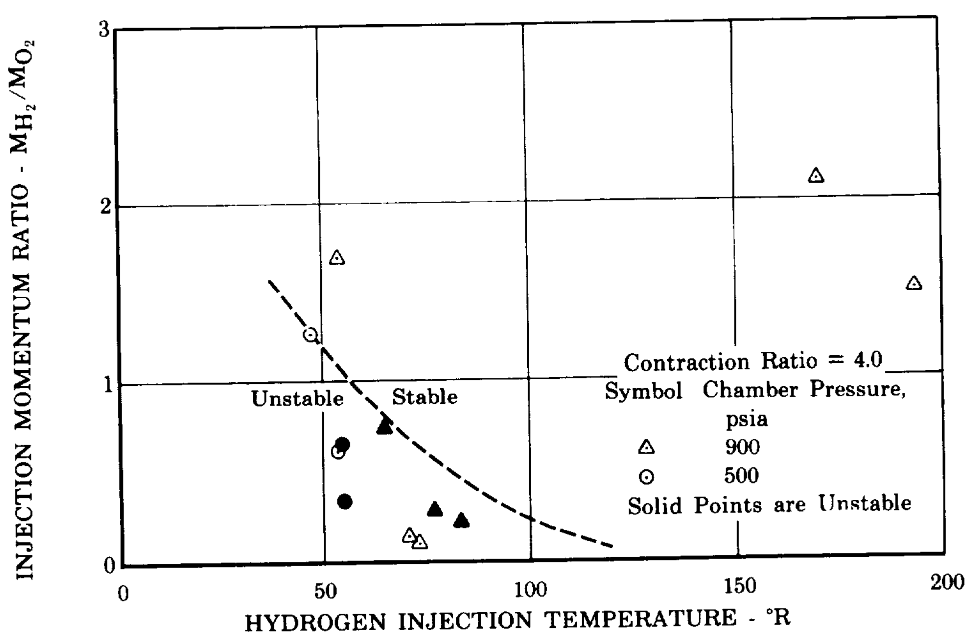

Figure IV-3. Indicated Effect of Injection Momentum Ratio and Hydrogen Temperature at a Contraction Ratio of 4.0 on Slab Motor Stability (Separated by Nominal Chamber Pressure) FD 11630

Figure IV-4 is a composite of the three curves previously presented, showing that the stable-unstable separation lines form a family of curves and give strong evidence of a contraction ratio effect. Consideration of all the data presented provides more substantive evidence of the general stabilizing effects of increased injection momentum ratio and increased fuel inlet temperature. Examination of this plot also indicates that no effect of chamber pressure is obvious for the test range of chamber pressure.

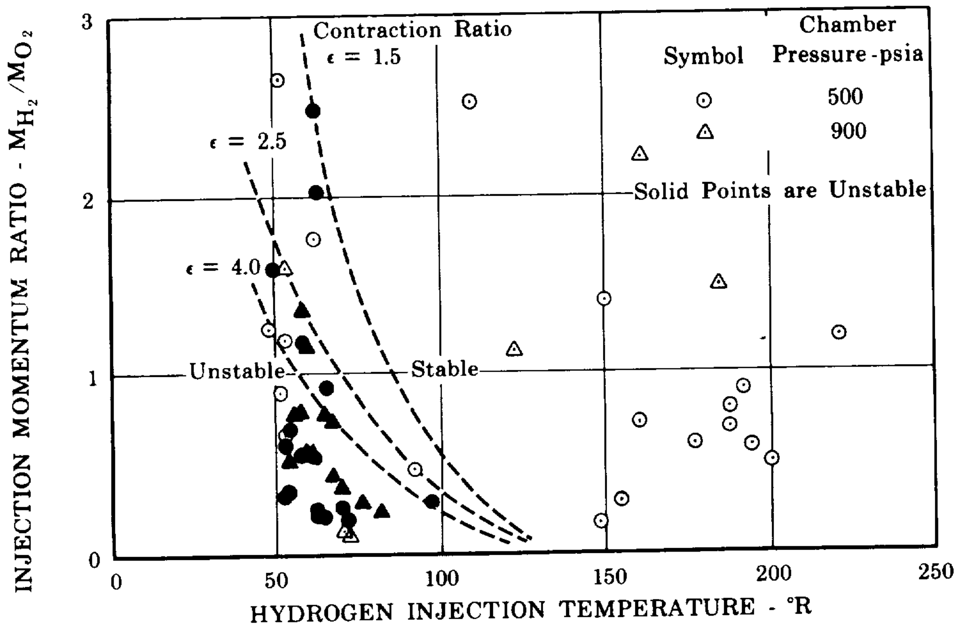

Figure IV-4. Injection Momentum Ratio vs Hydrogen Injection Temperature for Contraction Ratios of 1.5, 2.5, and 4.0 FD 11635

Data points at which low frequency chugging or intermediate frequency instability were experienced, but high-frequency instability was not present, are presented in figure IV-5 in relation to the stable-unstable separation lines previously discussed. No high-frequency unstable points are shown because chugging and high frequency instability were never experienced simultaneously, and high-frequency instability was usually accompanied by intermediate-frequency oscillations to a greater or lesser degree. The chugging points can be seen to generally occur in the region where no high-frequency instability is expected and therefore confirm the other test results. This also indicates that chugging is not likely to trigger high-frequency instability in otherwise stable regions.

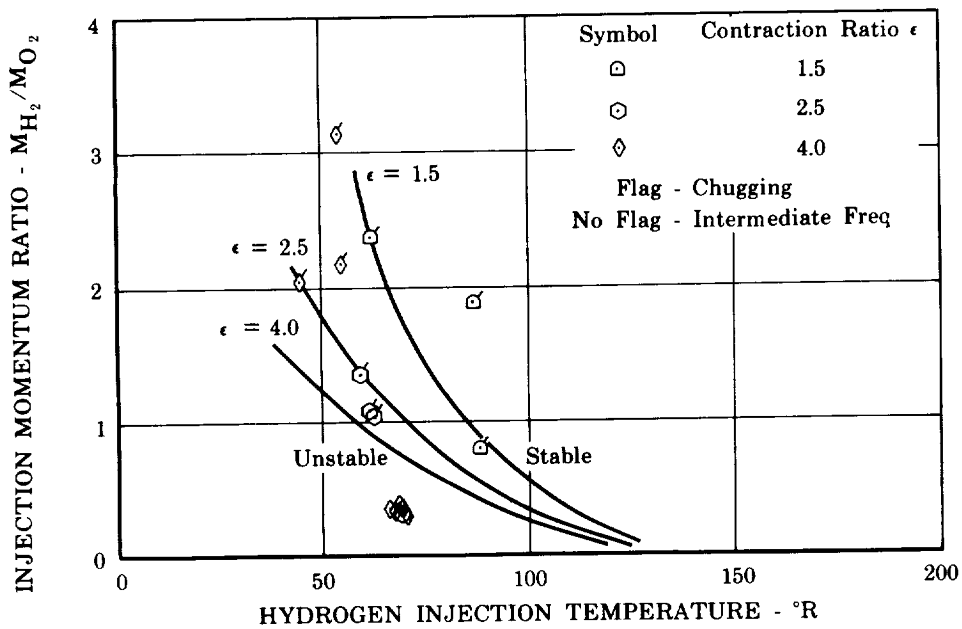

Figure IV-5. Data Points at which Low-Frequency Chugging or Intermediate-Frequency Instability were Experienced FD 11627

The intermediate-frequency points exist in the region where high-frequency instability would be expected. Although in many tests intermediate-frequency developed into high-frequency instability spontaneously or when pulsed, it may be that in some cases the presence of the intermediate-frequency disturbs the sustaining energy release process necessary for maintaining high-frequency instability.

Figure IV-6 presents Phase I slab motor data points in which swirlers were installed in the lower nine oxidizer injection elements. The presence of two unstable points indicates that this type of injector change can produce a radical shift in the stable-unstable separation line. This shift may have been caused by either the individual or combined effect of the swirlers and the unsymmetrical injector configuration resulting from swirlers in only half of the injection elements.

Data from tests conducted with the 10-inch diameter chamber and modified RL10 injector are presented in figure IV-7, including the stable-unstable separation lines previously shown. No pronounced effect of the change from the 1 x 5-inch slab motor to the 10-inch cylindrical chamber can be seen from these data. It is therefore believed that no significant difference would have been observed for the 5-inch diameter cylindrical chamber.

Further evaluation of the additional data correlations presented in Quarterly Report No. 2 (Reference 2) will be included in the final report.

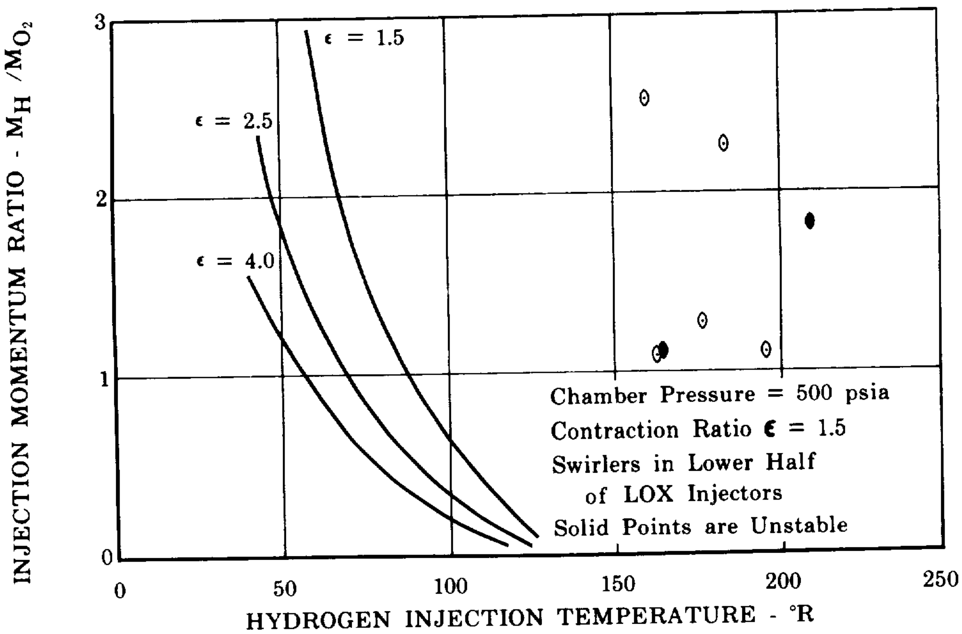

Figure IV-6. Phase I Slab Motor Data Points with Swirlers Installed in Lower Nine Oxidizer Injection Elements FD 11632

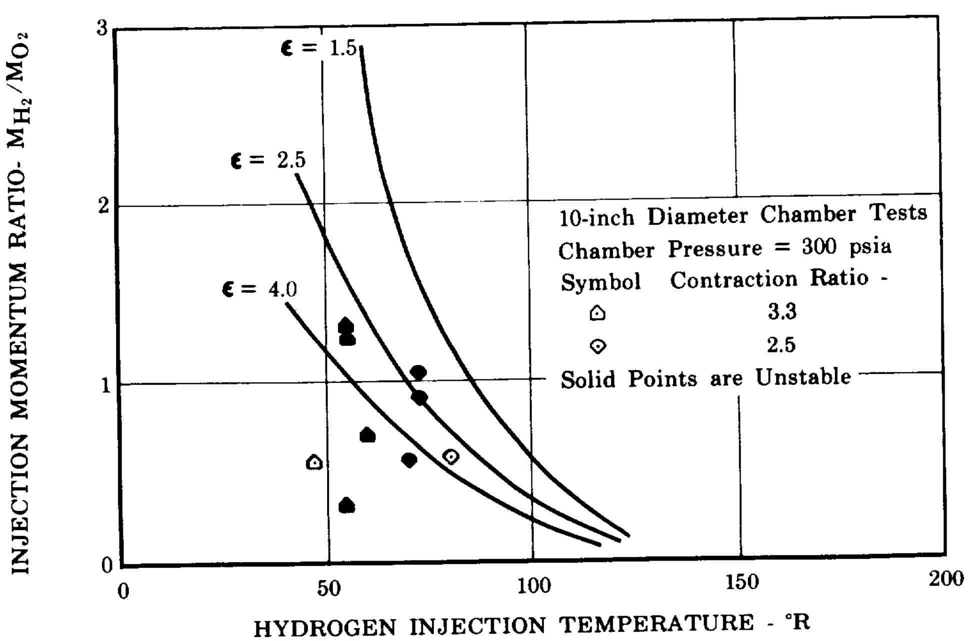

Figure IV-7. 10-inch Diameter Test Results FD 11634

SECTION V
FUTURE WORK

The following work is planned for the fourth quarter (16 March 1965 to 14 June 1965).

1. Assemble the 1 x 5-inch slab motor with 2.5 to 1 chamber contraction ratio nozzle inserts, sheet injector configuration, and test at 900 psia.

2. Reduce data and perform preliminary analysis of the above test results.

3. Complete analysis of all Phase I and Phase II test results.

4. Prepare final report and submit draft and approved final copies.

APPENDIX A
REFERENCES

1. Quarterly Progress Report No. 1, "Investigation of Combustion Instability with Liquid Oxygen and Liquid or Cold Gaseous Hydrogen Propellants," PWA FR-1117, 30 September 1964.

2. Quarterly Progress Report No. 2, "Ibid," PWA FR-1233, 30 December 1964.

COMBUSTION STABILITY

CONTRACT NAS 8-11024, MOD. 3

MANPOWER ESTIMATE

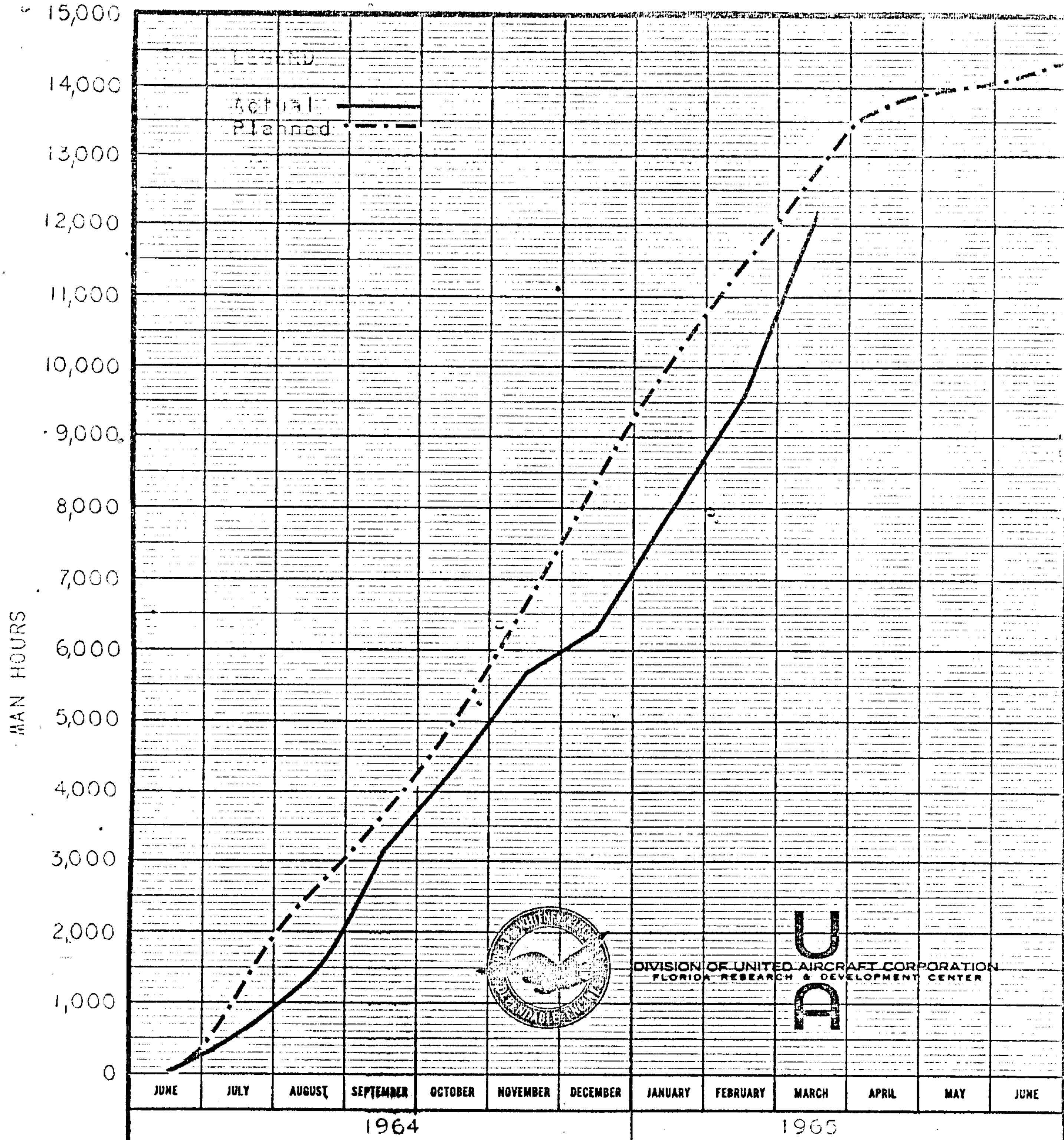

COMBUSTION STABILITY

CONTRACT NAS 8-11024, MOD. 3

FUNDING ESTIMATE

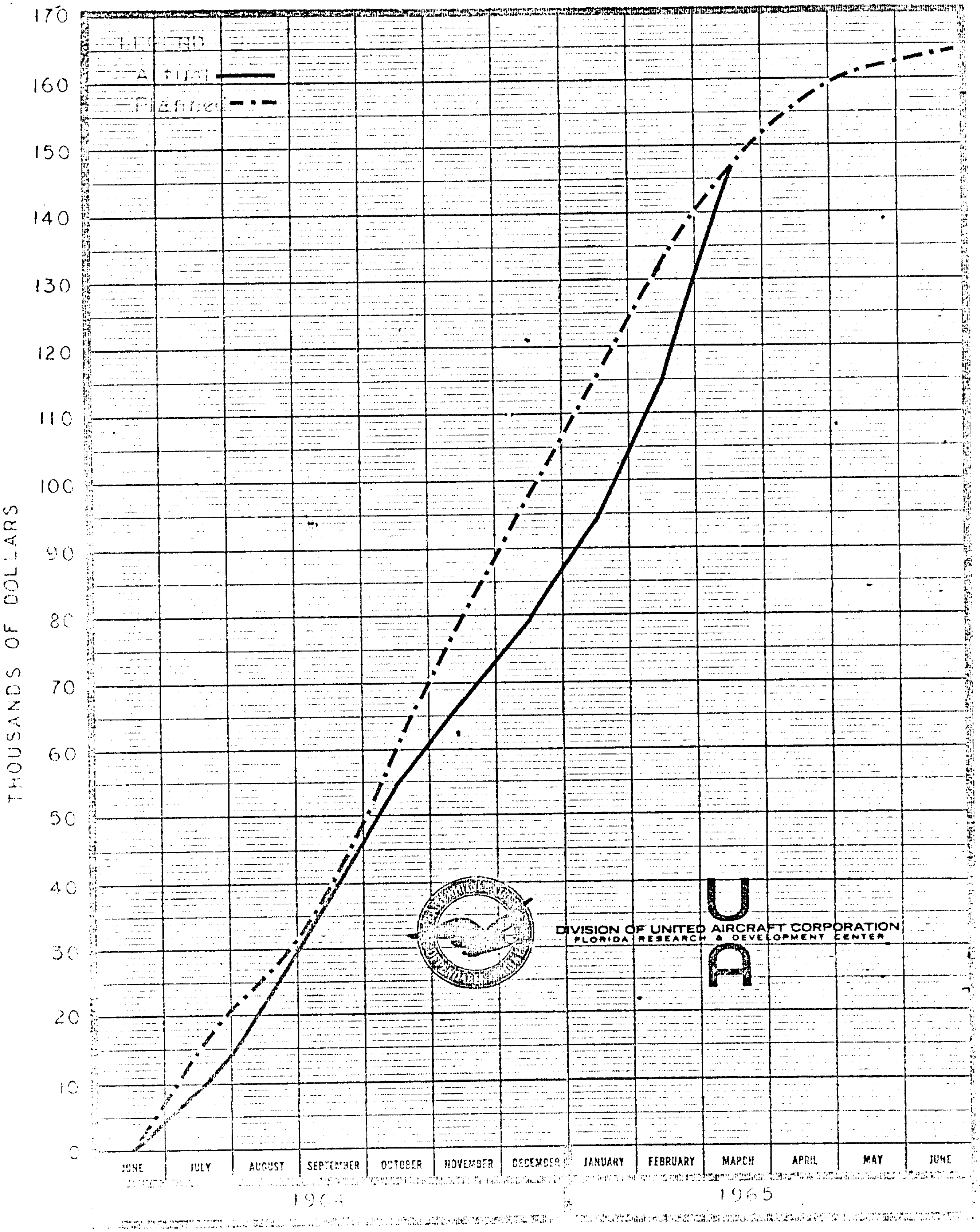

NOTE: ACTUAL COSTS ARE BASED ON PRELIMINARY DATA
(SEE NASA FORM 533 FOR REPORTED COSTS)